The Journal of Immunology

Adventitial Fibroblasts Induce a Distinct Proinflammatory/Profibrotic Macrophage Phenotype in Pulmonary Hypertension

Karim C. El Kasmi, Steven C. Pugliese, Suzette R. Riddle, Jens M. Poth, Aimee L. Anderson, Maria G. Frid, Min Li, Soni S. Pullamsetti, Rajkumar Savai, Maria A. Nagel, Mehdi A. Fini, Brian B. Graham, Rubin M. Tuder, Jacob E. Friedman, Holger K. Eltzschig, Ronald J. Sokol and Kurt R. Stenmark

J Immunol 2014; 193:597-609; Prepublished online 13 June 2014;
doi: 10.4049/jimmunol.1303048
http://www.jimmunol.org/content/193/2/597

The Journal of Immunology is published twice each month by
The American Association of Immunologists, Inc.,
1451 Rockville Pike, Suite 650, Rockville, MD 20852

Print ISSN: 0022-1767 Online ISSN: 1550-6606.

Adventitial Fibroblasts Induce a Distinct Proinflammatory/ Profibrotic Macrophage Phenotype in Pulmonary Hypertension

Karim C. El Kasmi,* Steven C. Pugliese,† Suzette R. Riddle,† Jens M. Poth,† Aimee L. Anderson,* Maria G. Frid,† Min Li,† Soni S. Pullamsetti,‡ Rajkumar Savai,‡ Maria A. Nagel,§ Mehdi A. Fini,† Brian B. Graham,¶ Rubin M. Tuder,¶ Jacob E. Friedman,‖ Holger K. Eltzschig,# Ronald J. Sokol,* and Kurt R. Stenmark†

Macrophage accumulation is not only a characteristic hallmark but is also a critical component of pulmonary artery remodeling associated with pulmonary hypertension (PH). However, the cellular and molecular mechanisms that drive vascular macrophage activation and their functional phenotype remain poorly defined. Using multiple levels of in vivo (bovine and rat models of hypoxia-induced PH, together with human tissue samples) and in vitro (primary mouse, rat, and bovine macrophages, human monocytes, and primary human and bovine fibroblasts) approaches, we observed that adventitial fibroblasts derived from hypertensive pulmonary arteries (bovine and human) regulate macrophage activation. These fibroblasts activate macrophages through paracrine IL-6 and STAT3, HIF1, and C/EBPβ signaling to drive expression of genes previously implicated in chronic inflammation, tissue remodeling, and PH. This distinct fibroblast-activated macrophage phenotype was independent of IL-4/IL-13–STAT6 and TLR–MyD88 signaling. We found that genetic STAT3 haplodeficiency in macrophages attenuated macrophage activation, complete STAT3 deficiency increased macrophage activation through compensatory upregulation of STAT1 signaling, and deficiency in C/EBPβ or HIF1 attenuated fibroblast-driven macrophage activation. These findings challenge the current paradigm of IL-4/IL-13–STAT6–mediated alternative macrophage activation as the sole driver of vascular remodeling in PH, and uncover a cross-talk between adventitial fibroblasts and macrophages in which paracrine IL-6–activated STAT3, HIF1α, and C/EBPβ signaling are critical for macrophage activation and polarization. Thus, targeting IL-6 signaling in macrophages by completely inhibiting C/EBPβ or HIF1α or by partially inhibiting STAT3 may hold therapeutic value for treatment of PH and other inflammatory conditions characterized by increased IL-6 and absent IL-4/IL-13 signaling. *The Journal of Immunology*, **2014, 193: 597–609.**

Studies in animal models of pulmonary hypertension (PH) and humans with pulmonary arterial hypertension (PAH) have provided convincing evidence that early and persistent inflammation is an essential component of pulmonary vascular disease (1–7). The extent of the vascular inflammatory infiltrate in PH was shown to correlate directly with parameters of vascular remodeling and hemodynamics (3, 4, 6). Importantly, as described extensively by our group (5, 8–12) and other investigators (3), PH-associated vascular inflammation is largely perivascular/adventitial in nature and is characterized by a robust influx of leukocytes, primarily macrophages, into the adventitial compartment. An essential role for these cells in the PH process was demonstrated in experiments in which in vivo depletion of macrophages attenuated pulmonary vascular remodeling (8). We documented that, in both experimental hypoxia-induced PH and human PAH, the pulmonary artery (PA) adventitia harbors activated

*Division of Gastroenterology, Hepatology, and Nutrition, Department of Pediatrics, School of Medicine, University of Colorado Denver, Aurora, CO 80045; †Division of Critical Care Medicine/Cardiovascular Pulmonary Research Laboratories, Department of Pediatrics and Medicine, School of Medicine, University of Colorado Denver, Aurora, CO 80045; ‡Department of Lung Development and Remodeling, Max-Planck Institute for Heart and Lung Research, University of Giessen and Marburg Lung Center, German Center for Lung Research, D-61231 Bad Nauheim, Germany; §Department of Neurology, University of Colorado Denver, School of Medicine, Aurora, CO 80045; ¶Program in Translational Lung Research, Department of Medicine, School of Medicine, University of Colorado Denver, Aurora, CO 80045; ‖Division of Biochemistry and Molecular Genetics, Department of Pediatrics, School of Medicine, University of Colorado Denver, Aurora, CO 80045; and #Department of Anesthesiology, School of Medicine, University of Colorado Denver, Aurora, CO 80045

Received for publication November 15, 2013. Accepted for publication May 6, 2014.

This work was supported in part by National Institutes of Health Axis Grant 1R01 HL114887-02, Program Project Grant 5P01 HL014985-39, and Training Grant 2T32 HL07171-36. J.M.P. was supported by Grant D/10/52531 from the German Academic Exchange Service.

K.C.E.K. and K.R.S. conceived the study, delineated the hypotheses, designed the study, analyzed and interpreted data, and prepared the manuscript; S.R.R., H.K.E., A.L.A., M.G.F., M.L., S.S.P., S.C.P., R.S., M.A.N., M.A.F., and J.M.P. acquired data, performed experiments, and provided reagents and technical assistance; and B.B.G., R.M.T., J.E.F., and R.J.S. were substantially involved in the preparation of the manuscript.

Address correspondence and reprint requests to Dr. Karim C. El Kasmi or Dr. Kurt R. Stenmark, Department of Pediatrics, Division of Gastroenterology, Hepatology, and Nutrition, University of Colorado Denver, School of Medicine, 12700 East 19th Avenue, Research Complex II, Aurora, CO 80045 (K.C.E.K.) or Department of Pediatrics and Medicine, Division of Critical Care Medicine/Cardiovascular Pulmonary Research Laboratories, University of Colorado Denver, School of Medicine, Aurora, CO 80045 (K.R.S.). E-mail addresses: Karim.Elkasmi@UCDenver.edu (K.C.E.K.) or Kurt.Stenmark@UCDenver.edu (K.R.S.)

The online version of this article contains supplemental material.

Abbreviations used in this article: AAM, alternative activation of macrophages; BMDM, bone marrow–derived macrophage; CM, conditioned medium (conditioned media); CO-Fib, fibroblast isolated from human or bovine control; CT, threshold cycle; dPA, distal pulmonary artery; iPAH, idiopathic pulmonary arterial hypertension; MCT, monocrotaline; PA, pulmonary artery; PAH, pulmonary arterial hypertension; P_B, barometric pressure; PBGD, porphobilinogen deaminase; PH, pulmonary hypertension; PH-Fibs, adventitial fibroblast isolated from calves with PH or humans with iPAH; siRNA, small interfering RNA; WT, wild-type.

fibroblasts (termed "PH-Fibs" in this article: adventitial fibroblast isolated from calves with PH or humans with iPAH) with a hyperproliferative, apoptosis-resistant, and proinflammatory phenotype (the last defined by increased generation of IL-6, IL-1β, CCL2/MCP1, CCL12/SDF1, VCAM1, osteopontin) that are involved in macrophage recruitment, retention, and activation (10, 12–17). We further demonstrated that the proinflammatory phenotype of PH-Fibs remains persistent ex vivo over numerous passages in culture and is regulated through epigenetic mechanisms involving alterations in histone deacetylase activity and microRNA expression (16, 17). In line with this paradigm, we found that PH-Fibs recruit, retain, and activate naive macrophages (17). However, neither the exact phenotype induced nor the signaling pathways involved in the polarization of macrophages in sterile forms of PH have been identified.

Tissue remodeling and fibrotic-angiogenic responses in chronic inflammatory conditions, including PH, have long been associated with alternative activation of macrophages (AAM) (12, 18–20). The current paradigm holds that IL-4/IL-13 signaling and STAT6-regulated AAM are important in the vascular remodeling process in some forms of PH and in other fibrosing/tissue-remodeling conditions in which Th2 responses are prominent (21–26). However, recent reports documented that STAT3 signaling also can play a key role in chronic inflammatory diseases in which tissue remodeling is prominent (27–34). Further, recent studies strongly support a spectrum model of macrophage activation in which macrophage phenotype is dependent on specific signals present in the inflammatory microenvironment, rather than simply classic "M1" versus "M2" (35).

IL-6 has been identified as a major activator of STAT3 signaling in macrophages, and IL-6–STAT3 signaling promotes an activation profile distinct from that in IL-4/IL-13–induced AAM (36–38). IL-6 signaling recently was shown to drive fibrosis and unresolved inflammation in the peritoneum in the absence of IL-4, IL-13, and TGFβ (39). Further, many reports documented increased serum and lung concentrations of IL-6 in patients with PAH (31, 40, 41). A pathogenic role for IL-6 in certain forms of PH is supported by observations that IL-6–knockout mice are protected from PH (32), whereas IL-6–transgenic mice develop spontaneous PH and vascular remodeling (30).

Thus, we sought to examine the hypothesis that certain forms of PH, including those associated with chronic hypoxia, are characterized by the presence of a fibroblast-activated macrophage that exhibits a unique phenotype dependent on IL-6 and STAT3 signaling and distinct from the canonical alternatively (IL-4/IL-13) activated macrophage phenotype. Our approach was to examine the phenotype of macrophages both in vivo using models of severe hypoxia-induced PH and patients with PAH and in vitro by examining the effects of fibroblasts derived from animals and humans with PH on macrophage phenotype signaling. In this article, we show that fibroblast-derived paracrine IL-6 and macrophage STAT3 in conjunction with HIF1α and C/EBPβ signaling, and not IL-4/IL-13–STAT6, are pivotal in mediating activation of macrophages by adventitial fibroblasts from the pulmonary hypertensive vessel. Further, these fibroblast-activated macrophages express genes previously implicated in the pathogenesis of PH and associated with chronic nonresolving and fibrosing tissue responses. Thus, fibroblast-mediated macrophage activation and STAT3, HIF1α, and C/EBPβ signaling downstream of IL-6 may be important elements underlying certain forms of PH.

Materials and Methods

Immunohistological/immunofluorescence staining and laser-capture microdissection

Frozen OCT-embedded sections of human lung specimens from control subjects (n = 4) and patients with idiopathic PAH (iPAH; n = 5) were provided by Dr. Barbara Meyrick (Transplant Procurement Center, Vanderbilt University, Nashville, TN) via the Pulmonary Hypertension Breakthrough Initiative funded by the Cardiovascular Medical Research Education Fund. Additional paraffin-embedded, human tissue (n = 5 donor controls and n = 5 iPAH) was provided by S.S.P. Patient descriptions for this tissue were provided previously (16). Immunostaining was performed according to standard protocols.

For laser-capture microdissection, human lung tissue specimens from subjects with iPAH (n = 8) or donor controls (n = 7), obtained during lung transplantation, were used. Tissue specimens were the same ones used in our previous study (16). Intrapulmonary arteries (50–100 μm diameter) were microdissected under optical control using the Laser microdissection device LMD6000 (Leica, Wetzlar, Germany) and collected in Eppendorf tubes containing RNA lysis buffer. Total mRNA was extracted from human microdissected vessels using an RNeasy Micro Kit (QIAGEN, Hilden, Germany). RT-PCR was performed using the iScript cDNA Synthesis Kit (Bio-Rad, Munich, Germany). Real-time PCR was performed using iQ SYBR Green Supermix, according to the manufacturer's instructions (Bio-Rad), and with an Mx3000P (Stratagene, Heidelberg, Germany). Intron-spanning primers were designed using sequence information from the National Center for Biotechnology Information database. Threshold cycle (Ct) values were normalized to the endogenous control (porphobilinogen deaminase [*PBGD*]).

The study protocol for tissue donation was approved by the Ethics Committee (Ethik Kommission am Fachbereich Humanmedizin der Justus Liebig Universität Giessen) of the University Hospital Giessen (Giessen, Germany), in accordance with National Law and with Good Clinical Practice/International Conference on Harmonization guidelines. Written informed consent was obtained from each patient or his/her next of kin (AZ 31/93).

Animals

One-day-old calves were exposed to hypobaric hypoxia (barometric pressure [P_B] = 445 mm Hg) for 2 wk (n = 7); age-matched controls (n = 7) were kept at ambient altitude (P_B = 640 mm Hg). Wistar-Kyoto rats (8 wk old) were exposed to hypobaric hypoxia (P_B = 380 mm Hg) for 4 wk (n = 9); age-matched controls (n = 9) were kept at ambient altitude. Monocrotaline treatment of rats (experimental group, n = 12, controls, n =12) were performed as described elsewhere (17). Standard veterinary care was according to institutional guidelines in compliance with Institutional Animal Care and Use Committee–approved protocols.

Bone marrow–derived macrophages

Mouse bone marrow–derived macrophages (BMDMs) were generated from *Il4*$^{-/-}$/*Il13*$^{-/-}$, *IL4ra*$^{-/-}$, *Stat6*$^{-/-}$, *Myd88*$^{-/-}$, *C/ebpβ*$^{-/-}$, *Stat3*$^{fl/fl}$;Tie2cre, *Stat3*$^{fl/+}$;Tie2cre, and *Stat3*$^{+/+}$;Tie2cre mice (a gift from Dr. P. Murray, St. Jude Children's Research Hospital, Memphis, TN); *Hif1a*$^{fl/fl}$;LysMcre were bred in-house. C57BL/6 and BALB/c mice were purchased from The Jackson Laboratory (Bar Harbor, ME). All mice were on a C57BL/6 background, with the exception of *Il4ra*$^{-/-}$ mice (BALB/c). Rat BMDMs were generated from Sprague-Dawley rats. Bovine BMDMs were isolated from healthy calves and grown in complete Iscove's DMEM with 20% FBS and human M-CSF (50 ng/ml). When bovine BMDM cultures were initiated from frozen bone marrow cells, live cells were obtained using negative column selection (Dead Cell Removal Kit; Miltenyi Biotec, Auburn, CA) and incubated for 24 h with human (due to limited availability of bovine-specific) cytokines, stem cell factor (50 ng/ml), IL-3 (20 ng/ml), and IL-6 (50 ng/ml) before exposure to M-CSF. All BMDMs were cultured in murine or bovine rM-CSF (100 ng/ml) for 7 d prior to use.

Adventitial fibroblasts

Adventitial fibroblasts from distal PAs (dPAs) of calves (control or with PH) were isolated by explant culture, as described (16, 17). Consistent with our previous observations (17), fibroblasts from chronically hypoxic hypertensive calves (PH-Fibs) were significantly smaller in size than were those from controls (CO-Fibs) and proliferated at markedly higher rates, as shown previously (16). The PH-Fibs used for study exhibited modest α-smooth muscle actin immunoreactivity, were negative for smooth muscle myosin, and were HSP-47–positive and vimentin-positive. At the time of study, these cells lacked expression of CD34, CD14, and CD68. Human adventitial fibroblasts were a kind gift from Dr. N.W. Morrell (University of Cambridge, London, U.K.). HFL-1 human fetal lung fibroblasts were purchased from American Type Culture Collection (Manassas, VA). Experiments were performed on cells at passages 4–10. Conditioned medium (CM) was collected from confluent fibroblast cul-

tures and used to treat BMDMs or the THP-1 monocyte cell line (American Type Culture Collection).

For Transwell (Corning, Tewksbury, MA) experiments, distal pulmonary arteries (1–3 mm outer diameter) were isolated from either control or pulmonary hypertensive calf lungs and left whole or were separated into medial and adventitial layers prior to dissecting into 3-mm^2 pieces for incubation in the upper chamber, above naive mouse BMDMs, for 16 h. Adjacent tissue pieces were used for whole and separated tissue. Three tissue pieces from each animal were used per experiment.

All cytokines were purchased from BD Biosciences (San Jose, CA), Cell Signaling (Danvers, MA), Miltenyi Biotec (San Diego, CA), eBioscience (San Diego, CA), or Kingfisher Biotech (St Paul, MN). Ultrapure LPS was purchased from Sigma (St. Louis, MO).

Immunoblotting

Cells were lysed in M-PER Mammalian Protein Extract Reagent containing protease and phosphatase inhibitors (Thermo-Fisher, Waltham, MA). Protein lysates were separated by 4–15% gradient SDS-PAGE in Tris-HCl buffer and transferred to nitrocellulose membranes. Membranes were blocked in 3% milk in TBS containing 0.05% Tween. Abs included mouse monoclonal anti-ARG1 Ab (1:2000, BD Biosciences); rabbit polyclonal anti-total STAT1, p-STAT1, total STAT3, p-STAT3, total STAT6, p-STAT6 (1:1000; all from Cell Signaling Technology); and mouse monoclonal anti-GAPDH (1:1000, Santa Cruz, Dallas, TX).

IL-6 protein detection

Human IL-6 was quantified in cell culture supernatant using a human IL-6 multiplex sandwich ELISA with electrochemiluminescence detection on the MSD Platform, as per the manufacturer's protocol, on a SECTOR Imager 2400A (both from MESO SCALE DISCOVERY, Rockville, MD). Quantitative detection range for IL-6 in our analysis was 0.6 to 9871.4 pg/ml. Bovine IL-6 was quantified using an ELISA development kit (Kingfisher Biotech), according to the manufacturer's instructions and standard ELISA procedures. Bovine rIL-6 was used as a standard.

Quantitative RT-PCR

RNA was isolated using TRIzol reagent (Invitrogen, Grand Island, NY) or the QIAGEN RNeasy Kit (Valencia, CA), according to the manufacturer's instructions. First-strand cDNA synthesis was performed using an iScript cDNA Synthesis Kit (Bio-Rad, Hercules, CA). Quantitative RT-PCR was performed using TaqMan probes and reagents (Applied Biosystems, Grand Island, NY), according to the manufacturer's instructions. Gene expression was calculated after normalization to *Hprt1* using the Δ/Δ Ct method.

Statistical analysis

GraphPad Prism software was used to determine significance. Student *t* test was used to compare two groups. One-way ANOVA and Bonferroni correction for multiple comparisons were used to compare more than two groups.

Results

Expression of the STAT3-regulated proteins CD163 and CD206 on macrophages is observed in vivo in humans and animals with PH

We first sought to define the adventitial macrophage phenotype in situ in humans, as well as in several animal models of PH. Macrophage CD163 and CD206 expression was reported in various chronic inflammatory/fibrotic tissue responses (42, 43). CD163 is a STAT3-regulated gene (44), and CD206 can be activated through either IL-6–STAT3 or IL-4–STAT6 (Supplemental Fig. 1A). Thus, we chose to examine in situ expression of CD163 and CD206 on adventitial macrophages. Consistent with previous reports, we detected pronounced adventitial accumulation of macrophages (defined as cells positive for the pan-macrophage marker CD68) in the PA of patients with iPAH, calves with hypoxia-induced PH, and rats with hypoxia- or monocrotaline (MCT)-induced PH (Supplemental Fig. 1B, 1C) (3–6). Furthermore, the PAs of humans, calves, and rats with PH revealed markedly increased numbers of $CD163^+$ cells, which were specifically localized to the adventitia (Fig. 1A, Supplemental Fig. 1C). To attribute CD163 and CD206 staining to macrophages, the PA adventitia from calves with hypoxia-induced PH was stained with the typical macrophage marker MHC class II. Approximately 90% of $MHCII^+$ cells coexpressed the macrophage-specific marker CD68, as detected by double staining and confocal microscopy. In addition, the majority (75%) of $CD163^+$ and $CD206^+$ cells also coexpressed MHC class II (Supplemental Fig. 1D). $CD163^+$ cells in the PA adventitia from calves with hypoxia-induced PH also expressed the canonical STAT3-regulated protein SOCS3 (Supplemental Fig. 1E). Moreover, we detected increased adventitial protein expression of p-STAT3 in PAs from patients with iPAH (Fig. 1B), which was paralleled by the detection of increased mRNA (obtained by laser-capture microdissection) of the canonical STAT3-regulated genes *SOCS3* and *IL4Ra* (Fig. 1C), together with increased protein and mRNA expression of the STAT3-activating cytokine IL-6 (Fig. 1B, 1C). Notably, we did not detect mRNA for the STAT6-activating cytokines *IL4* or *IL13* in PAs from calves, humans, or rats with PH (data not shown).

These results demonstrate that, in various species and multiple models of PH, macrophages consistently accumulate within the PA adventitia, the site of active vascular remodeling, and stereotypically express surface markers associated with a proremodeling phenotype, consistent with activation through IL-6–STAT3 signaling.

Adventitial fibroblasts mediate macrophage activation

We next sought to determine the cell type(s) and mechanism(s) responsible for macrophage activation toward this phenotype, hypothesizing that the PA adventitia was the vascular compartment most capable of activating these macrophages. Exposure of naive primary BMDMs in vitro to intact whole PA explants from calves with hypoxia-induced PH significantly increased transcription of *Cd163*, *Cd206*, *Il4ra*, and *Socs3* (Fig. 2A). Removal of adventitia from the PA explant resulted in a marked decrease in mRNA expression in BMDMs. However, the adventitia alone induced an identical response to that observed with whole PA explants (Fig. 2A). These findings were confirmed in a separate experiment using bovine BMDMs (data not shown). These results demonstrate that during vascular remodeling in PH, cells within the remodeled PA adventitia produce soluble factors that can activate primary naive macrophages toward a gene expression phenotype that is identical to the one observed on adventitial macrophages in situ.

To test whether proinflammatory PA adventitial fibroblasts (16, 17) were the cellular source of soluble factors inducing this macrophage phenotype, we exposed naive BMDMs to CM generated by ex vivo–cultured human (from patients with iPAH) or bovine (from calves with hypoxic PH) adventitial fibroblasts (PH-Fibs). Remarkably, CM from both bovine and human PH-Fibs significantly increased transcription of *Cd163*, *Cd206*, *Socs3*, and *Il4ra* in naive macrophages (mouse and bovine) and THP-1 monocytes in comparison with that induced by CM from CO-Fibs. Additionally, CM from bovine PH-Fibs induced similar gene expression in mouse and rat (data not shown) naive macrophages, indicating that this signaling mechanism is effective across species (Fig. 2B, Supplemental Fig. 2). Thus, within the remodeled PA adventitia of animals and humans with PH, activated fibroblasts provide the soluble factors that induce this macrophage phenotype.

Fibroblast-activated adventitial macrophages do not exhibit a canonical alternatively activated phenotype

Macrophage expression of CD163 and CD206 in fibrosis and tissue remodeling is thought to reflect a canonical AAM phenotype (42, 45, 46), as defined by IL-4/IL-13/IL-4Rα/STAT6–dependent signaling (47). Therefore, we sought to determine whether the functional programming of adventitial macrophages by the PA adventitia and PA adventitial fibroblasts involved IL-4/IL-13/IL-4Rα/STAT6 signaling.

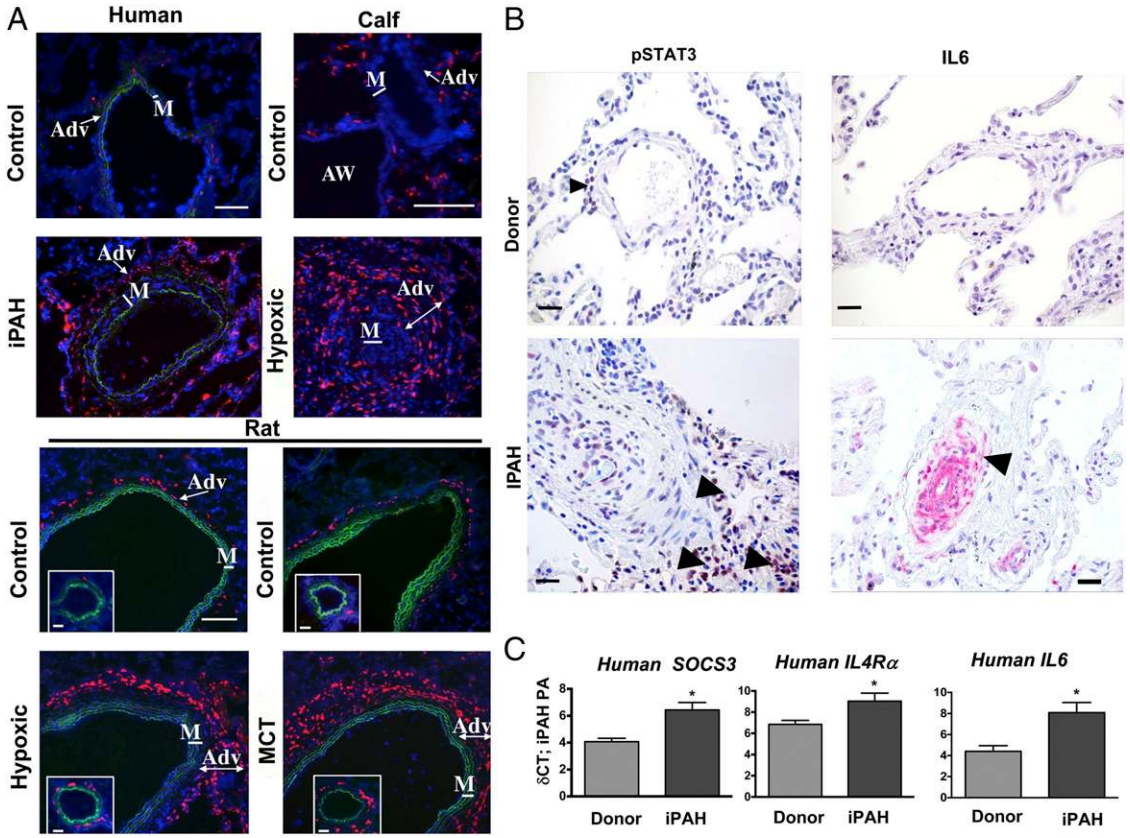

FIGURE 1. In various forms of PH, adventitial macrophages express CD163. (**A**) Accumulation of $CD163^+$ (human, calf) and $ED2^+$ (CD163 analog in rats) cells (red fluorescence) in human, calf, and rat PAs. Note localization to the PA adventitia (Adv, shown by arrows). All panels show DAPI counterstain (cell nuclei, blue) and autofluorescence of vascular elastic lamellae (green) defining borders of vascular media. Cryosections of intralobar PAs were immunostained. Scale bars, 100 μm. (**B**) Immunostaining for p-STAT3 (brown) and IL-6 (pink) in formalin-fixed tissue from patients with iPAH, and donor(s) as controls. Note adventitial staining for p-STAT3 and IL-6 in PA from patients with iPAH (arrowheads). Images are representative of eight patients and five donors. Scale bars, 20 μm. (**C**) Gene expression of canonical macrophage STAT3-regulated genes *IL4Ra* and *SOCS3*, as well as the STAT3 inducer *IL6*, in laser-capture microdissected PA tissue from humans with iPAH and controls (Donor; both $n = 8$), expressed as δCt values normalized to expression of PBGD. $*p < 0.05$, paired two-tailed Student *t* test. Control human donors or normoxic animals; iPAH, idiopathic pulmonary arterial hypertension; M, media of PA; MCT, MCT-induced PH.

Accordingly, we examined transcription of canonical STAT6-regulated genes whose combined expression in macrophages has traditionally been viewed to reflect the AAM phenotype (*Arg1* encoding Arginase1, *Chi3l3* encoding chitinase-3-like protein 3/YM1, and *Retnla* encoding resistin-like molecule Relmα/FIZZ1) (19, 47). We discovered that soluble factors released by intact whole PA explants or by isolated PA adventitia (both containing fibroblasts) derived from calves with chronic hypoxia–induced PH significantly increased transcription of *Arg1*, but not of *Chi3l3* and *Retnla*, in mouse macrophages. PA explants from which the adventitia was removed (absence of fibroblasts) failed to induce significant expression of any gene (Fig. 3A). In addition, CM produced by PH-Fibs replicated this gene expression pattern in mouse, rat, and bovine BMDMs (Fig. 3B, 3C, Supplemental Fig. 3A). The absence of *Chi3l3* and *Retnla* mRNA induction in mouse macrophages was not due to an inability to respond to IL-4 and also was not limited to a particular time point (Supplemental Fig. 3B).

Furthermore, compared with CO-Fibs, neither human nor bovine PH-Fibs had increased transcription for *IL4* or *IL13* and neither human nor bovine PH-Fib CM contained detectable amounts of IL-4 or IL-13 protein (data not shown). In addition, neither bovine nor human PH-Fib CM induced transcription of another canonical STAT6-regulated AAM gene, *TGM2/Tgm2* (data not shown). Moreover, we discovered that PH-Fib CM induced Arginase1 protein expression in mouse, rat, and bovine macrophages in the absence of STAT6 phosphorylation but in the presence of STAT3 phosphorylation (Supplemental Fig. 3C–E). Additionally, *Arg1* mRNA expression in PH-Fib CM–activated macrophages did not require paracrine or autocrine IL4/IL-13 signaling, because expression of *Arg1* was similar in macrophages from IL-4/IL-13 double-deficient mice (unresponsive to autocrine IL-4/IL-13), $Il4Ra^{-/-}$ mice (unresponsive to paracrine and autocrine IL-4 and IL-13), and STAT6-deficient mice (unable to upregulate *Arg1* in response to IL-4/IL-13) in response to bovine PH-Fib CM (Fig. 3D). Because *Arg1* also can be induced in response to TLR–MyD88 signaling (48) and C/EBPβ signaling (36, 48, 49), we exposed naive mouse macrophages from wild-type (WT), $Myd88^{-/-}$, and $C/ebpb^{-/-}$ mice to bovine PH-Fib CM. Although *Arg1* expression was similar in WT and $MyD88^{-/-}$ macrophages (Fig. 3E), $C/ebpb^{-/-}$ macrophages showed dramatically reduced *Arg1* expression (Fig. 3F). These results demonstrate that PH-Fib–activated macrophages were not alternatively activated through the IL-4/IL-13–STAT6 pathway and that neither the IL-4/IL-13/IL-4R/STAT6 pathway nor the MyD88 (microbe- and danger-associated signals and IL1) pathway underlies *Arg1* expression; instead, STAT3 and C/EBPβ play a critical role.

PH-Fibs activate macrophages through paracrine IL-6

Because IL-6 activates STAT3 signaling in macrophages, which, in turn, can activate C/EBPβ (36, 37), we next examined whether

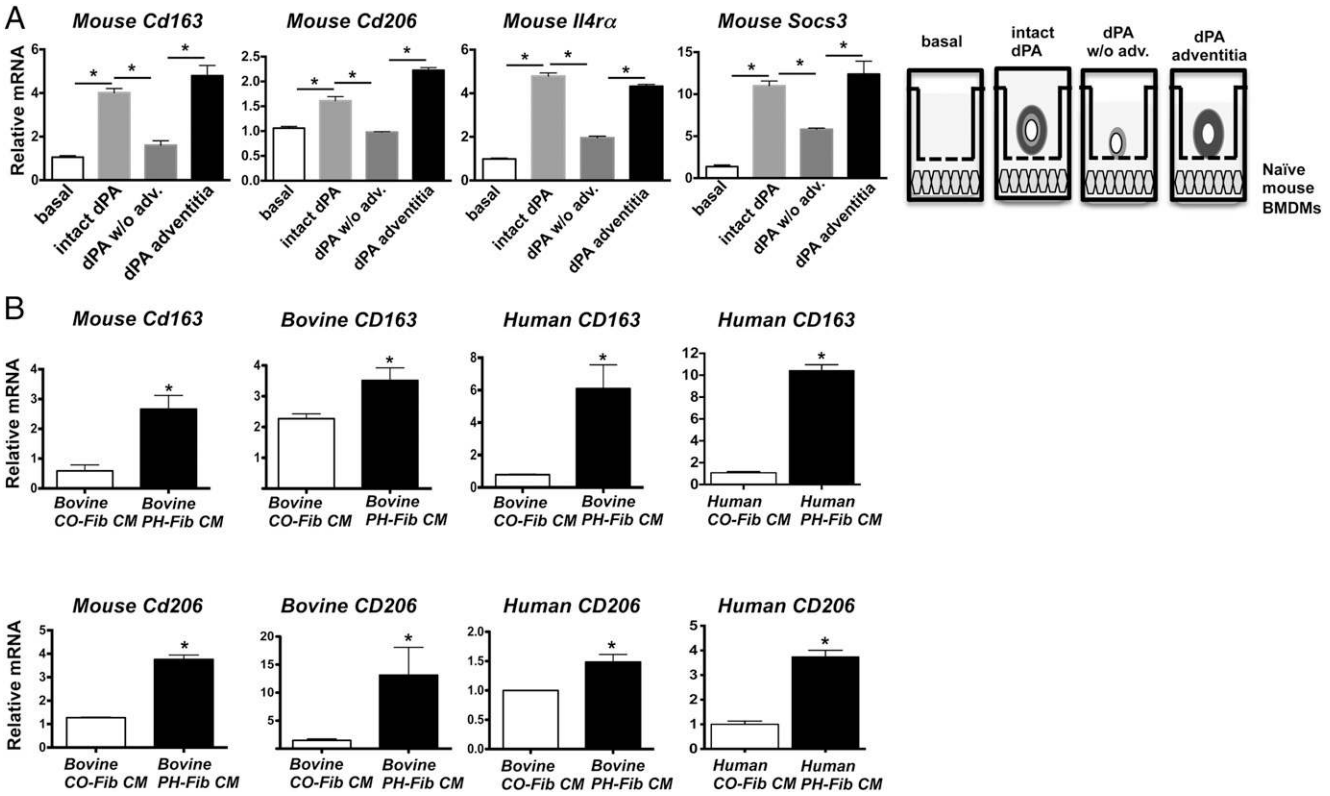

FIGURE 2. Adventitial fibroblasts activate macrophages. (**A**) Transwell experiment depicting mRNA expression in mouse BMDMs exposed to soluble factors generated by dPA explants from calves with chronic hypoxia–induced PH. dPAs were isolated, and as depicted in the diagram, an intact piece of PA tissue (intact dPA), a PA tissue piece from which the adventitia had been removed (dPA w/o adv.), and the removed adventitia piece itself (dPA adventitia) were incubated in the upper chamber of a 0.4-μm Transwell in the presence of naive mouse BMDMs (lower chamber) for 16 h prior to RNA isolation and quantitative RT-PCR. Displayed is the fold induction (normalized to basal expression) of a representative PCR triplicate (average ± SEM) from one of two calves. Three dPA segments were tested from each animal. *$p < 0.05$, one-way ANOVA. (**B**) Gene expression in BMDMs or monocytes exposed to CM from dPA adventitial fibroblasts (PH-Fibs or CO-Fibs). CM from ex vivo–cultured bovine PH-Fibs (PH-Fib CM), and not from controls (CO-Fib CM), promotes gene expression of *Cd163* (*upper left panels*) and *Cd206* (*lower left panels*) in naive mouse and bovine BMDMs. CM from bovine and human PH-Fibs induce expression of *CD163* (*upper right panels*) and *CD206* (*lower right panels*) in naive human THP-1 monocytes after 16 h of exposure. Relative mRNA levels are presented as mean ± SEM of PCR triplicates after normalization to *Hprt1* expression and relative to gene expression in untreated macrophages/monocytes (basal) and are representative of $n \geq 5$ experiments with CM from at least three PH-Fib and CO-Fib populations isolated from at least three animals/patients and using BMDMs from at least three animals. *$p < 0.05$, unpaired two-tailed Student *t* test.

paracrine, fibroblast-derived IL-6 could be responsible for the macrophage activation. Increased IL-6 and p-STAT3 protein expression in the PAs from patients (Fig. 1B), along with evidence of STAT3 signaling in adventitial macrophages (Supplemental Fig. 1E [SOCS3 staining], Supplemental Fig. 4), supported the idea that IL-6 was the most likely paracrine cytokine to activate STAT3 signaling in fibroblast-activated macrophages. We found that adventitial fibroblasts from calves with PH generated IL-6 protein and *IL6* mRNA (Fig. 4A). Small interfering RNA (siRNA) knockdown of *IL6* expression in bovine PH-Fibs led to a reduction in IL-6 protein in the CM (Fig. 4B), which resulted in significant attenuation of the CM-induced transcriptional upregulation of STAT3-regulated genes in naive mouse macrophages (Fig. 4C). In addition, expression of these genes was not reduced in IL-6–deficient macrophages in response to PH-Fib CM (Fig. 4D), ruling out any potential contribution of autocrine IL-6 signaling to the activation of STAT3 signaling in fibroblast-activated macrophages.

PIM1 and NFATC2 signaling is promoted in fibroblast-activated macrophages

We next tested whether this IL-6–STAT3–regulated fibroblast-activated macrophage phenotype would also include expression of additional functional STAT3-regulated genes that have previously been associated with the pathogenesis of PH, such as *Pim1*, and *Nfatc2* (33, 34). Gene expression analysis using laser-capture microdissection of PAs from patients with iPAH revealed upregulation of mRNA for *PIM1* and *NFATC2* (Fig. 5A). In addition, intact whole PA and PA adventitia from PH calves induced transcription of *Pim1* and *Nfatc2* in naive mouse macrophages (Fig. 5B). Moreover, bovine PH-Fib CM induced *Pim1* and *Nfatc2* expression in naive bovine (Fig. 5C), mouse (Fig. 5D), and rat (Fig. 5E) macrophages. Human PH-Fib CM also was capable of inducing transcription of *PIM1*, but not *NFATC2*, in human monocytes (data not shown). PH-Fib CM–induced expression of *Pim1* and *Nfatc2* was dependent on paracrine IL-6 but not autocrine IL-6 (Fig. 5F, 5G). Finally, transcriptional induction of *Pim1*, *Nfatc2*, *Socs3*, and *Il4ra* mRNA in mouse macrophages activated by bovine PH-Fib CM was independent of STAT6 or MyD88 (experiments performed in *Stat6*$^{-/-}$ and *MyD88*$^{-/-}$ BMDMs) (data not shown).

PH-Fib–activated macrophages demonstrate upregulated Hif1*a and* Vegfa *mRNA*

HIF1 can be induced through STAT3 (50). Gene expression analysis of PAs from patients with iPAH revealed upregulation of *HIF1A* mRNA (Fig. 6A). Mouse macrophages exposed to whole intact PA and PA adventitia from calves with hypoxia-induced PH showed increased *Hif1a* mRNA expression (Fig. 6B). Bovine PH-Fib CM also induced transcription of *Hif1a* in naive mouse, rat, and

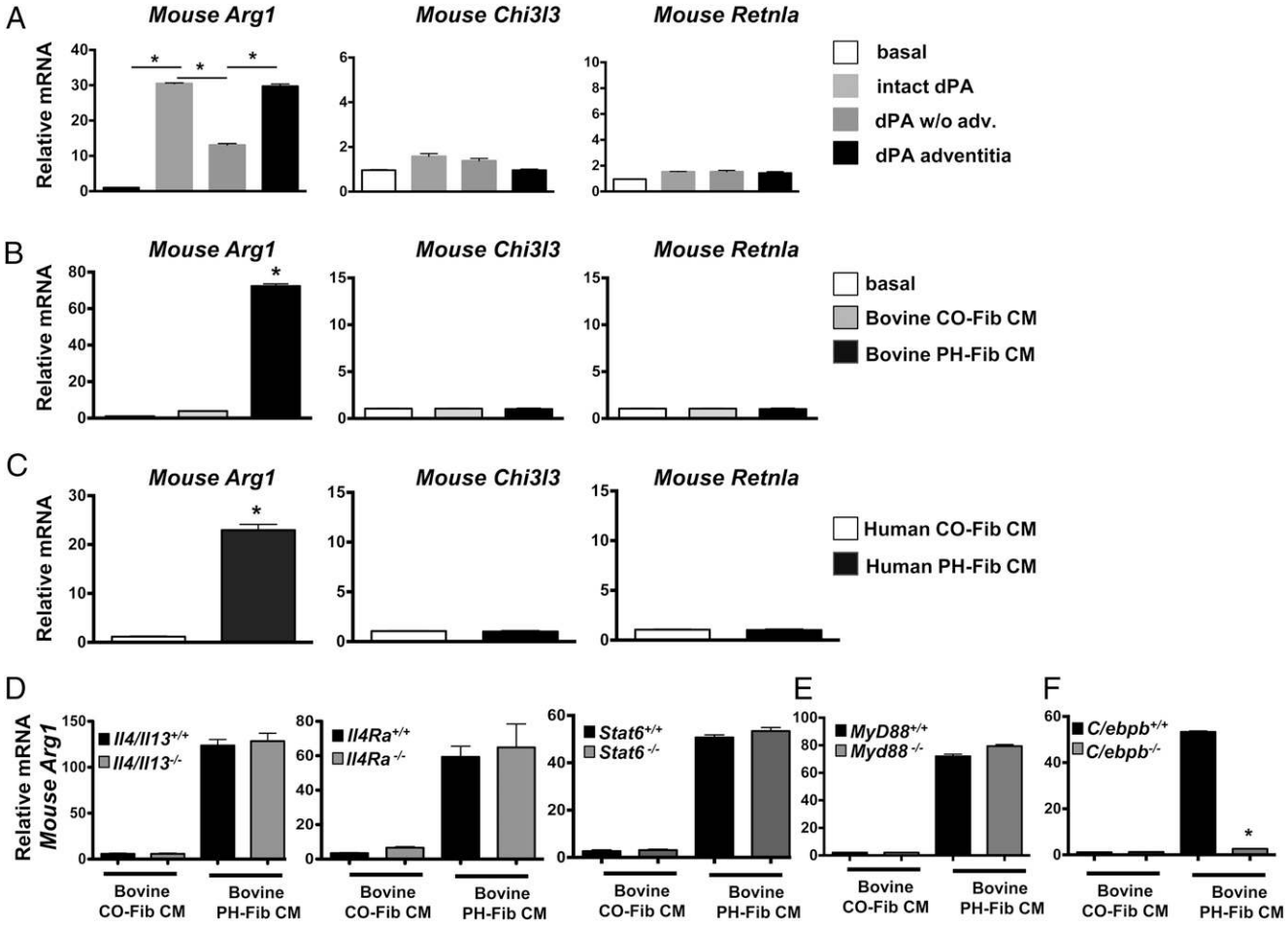

FIGURE 3. Fibroblast-activated adventitial macrophages do not exhibit a canonical alternatively activated phenotype. (**A**) Soluble factors from the dPA adventitia (using dPA explants and 0.4-μm Transwells as in Fig. 2 diagram) induce gene expression of *Arg1*, but not *Chi3l3* and *Rentla*, in mouse BMDMs. Displayed is the fold induction (normalized to basal expression) of a representative PCR triplicate (average ± SEM) from one of two calves. Three dPA segments were tested from each animal. *$p < 0.05$, one-way ANOVA. (**B** and **C**) PH-Fib CM, but not CO-Fib CM, induce *Arg1*, but not *Chi3l3* or *Rentla*, gene expression in mouse BMDMs (16-h time point shown). The effect is similar with CM generated from bovine (B) or human (C) PH-Fibs and CO-Fibs. Data are mean ± SEM of PCR triplicates after normalization to expression of *Hprt1* and relative to gene expression in untreated macrophages (basal). The results from representative PH-Fib CM and CO-Fib CM samples are shown, obtained from three cell populations (from different calves/patients) of each cell phenotype that were tested at least three times on BMDMs generated from at least three mice. *$p < 0.05$, unpaired two-tailed Student *t* test. (**D** and **E**) Bovine PH-Fib CM induce comparable transcript levels for *Arg1* in WT BMDMs and BMDMs derived from *Il4/Il13*$^{-/-}$, *Il4ra*$^{-/-}$, *Stat6*$^{-/-}$, and *Myd88*$^{-/-}$ mice. (**F**) *Arg1* expression in WT BMDMs is significantly attenuated in response to PH-Fib CM in BMDMs from *C/ebpb*$^{-/-}$ mice. PCR data in (D)–(F) are mean ± SEM from PCR triplicates after normalization to expression of *Hprt1* (16-h time point) and expressed relative to gene expression in untreated BMDMs (basal). Displayed are findings representative of experiments with CM from three PH-Fib and three CO-Fib populations repeated on BMDMs from three animals. *$p < 0.05$, one-way ANOVA.

bovine macrophages (Fig. 6C–E). Human PH-Fib CM also induced *HIF1A* mRNA in naive human monocytes (Fig. 6F). Notably, in mouse macrophages, this response was independent of autocrine IL-6, STAT6, and MyD88 (experiments performed in *Il6*$^{-/-}$, *Stat6*$^{-/-}$, and *MyD88*$^{-/-}$ BMDMs), as well as hypoxia (experiments conducted under normoxic conditions) (data not shown).

HIF1 regulates expression of VEGFA, which has been implicated in the pathogenesis of PH. Mouse macrophages exposed to whole intact PA and PA adventitia from calves with hypoxia-induced PH showed increased *Vegfa* mRNA expression (Fig. 7A). Bovine PH-Fib CM also induced transcription of *Vegfa* in naive mouse, rat, and bovine macrophages (Fig. 7B–D). Human PH-Fib CM also induced *VEGFA* mRNA in naive human monocytes (Fig. 7E).

STAT3, HIF1α, and C/EBPβ are critical regulators of PH-Fib–mediated macrophage activation

The above results suggested that STAT3, C/EBPβ, and HIF1 are central regulators of the fibroblast-activated and IL-6–activated macrophage phenotype. Therefore, we examined their role in fibroblast and IL-6–mediated macrophage activation by using a genetic approach. We first examined the role of STAT3 and used BMDMs from mice with conditional alleles of *Stat3* (*Stat3*$^{fl/fl}$ [complete knockout] and *Stat3*$^{fl/+}$ [haplodeficiency, incomplete knockout]) crossed onto the Tie2cre background [mice lacking *Stat3* globally are embryo lethal (51)]. As expected, BMDMs with haplodeficiency in STAT3 (from *Stat3*$^{fl/+}$; *Tie2Cre* mice) displayed attenuated activation, as reflected by ∼50% reduction in gene expression of STAT3 target genes in response to PH-Fib CM and bovine rIL-6 (Fig. 8A) and mouse rIL-6 (data not shown). Unexpectedly, expression of STAT3 target genes was not attenuated in BMDMs with complete absence of STAT3; instead, it was increased in response to bovine PH-Fib CM (Fig. 8A). As reported previously, IL-6 stimulates STAT1 signaling in murine fibroblasts with complete genetic absence of STAT3 (52). Thus, we determined STAT1 and STAT3 signaling in WT BMDMs, in response to either IL-6 or PH-Fib CM, and found that STAT1 was weakly

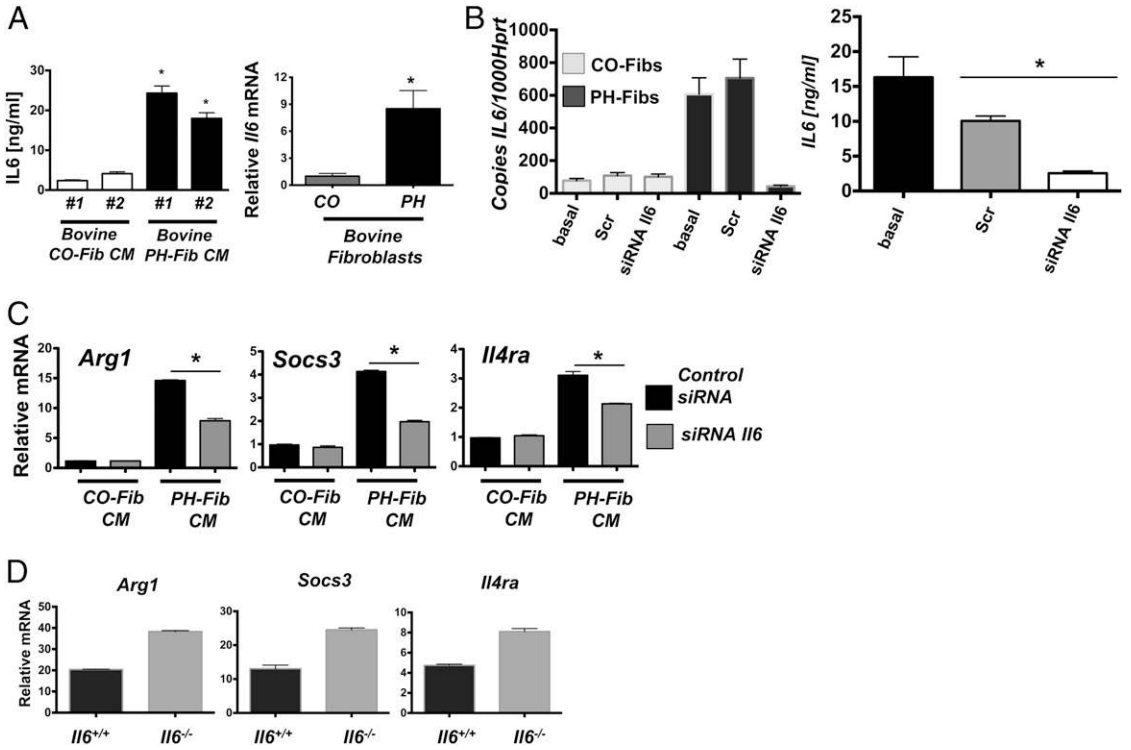

FIGURE 4. PH-Fibs activate macrophages through paracrine IL-6. (**A**) IL-6 protein amounts (*left panel*) in CM from two bovine PH-Fib populations; mean ± SEM of technical triplicates of individual biological samples (two CO-Fibs and two PH-Fibs populations) are shown. $*p < 0.05$ versus CO-Fib CM, Student *t* test. Relative *IL6* mRNA (*right panel*) in bovine CO-Fibs (normalized to 1, $n = 5$) and in PH-Fibs ($n = 4$). $*p < 0.05$ versus CO-Fibs, Student *t* test. (**B**) siRNA-mediated knock down of *IL6* transcription in bovine CO-Fibs and PH-Fibs (*left panel*) and IL-6 protein amounts (ELISA assay, *right panel*) in CM from untreated (basal), scrambled (Scr), and IL-6 siRNA–treated PH-Fibs ($n = 3$ each) tested in triplicate; mean ± SEM is shown from analysis of triplicate samples and is representative of two separate experiments. $*p < 0.05$. (**C**) siRNA-mediated suppression of *IL6* gene transcription in bovine PH-Fibs limits the ability of CM to induce transcription of STAT3-regulated genes in WT mouse BMDMs. Gene expression is normalized to expression of *Hprt1* and relative to that in macrophages exposed to CM from CO-Fibs treated with control siRNA. Data are mean ± SEM from triplicate determinations and are representative of two separate experiments. $*p < 0.05$. (**D**) Expression of STAT3-regulated genes in *WT* and $Il6^{-/-}$ BMDMs exposed for 16 h to bovine PH-Fib CM. One representative experiment with CM from one of three PH-Fib populations was tested on BMDMs from three animals of each genotype.

phosphorylated and, as expected, STAT3 was strongly phosphorylated, demonstrating that IL-6R can initiate both STAT3 and STAT1 signaling (Supplemental Fig. 4A). Consistent with this finding and the previously reported data in mouse $Stat3^{-/-}$ fibroblasts, we found that, in BMDMs with complete genetic absence of *Stat3*, both IL-6 and PH-Fib CM induced increased and prolonged STAT1 phosphorylation in the absence of STAT3 phosphorylation (Supplemental Fig. 4A). Moreover, PH-Fib CM induced significantly higher transcript levels of the canonical STAT1-regulated genes *Ip10* and *Irf1* in BMDMs with complete STAT3 deficiency compared with WT macrophages (Fig. 8B). In addition, in BMDMs with complete STAT3 deficiency, expression of *Ip10* and *Irf1* mRNA was increased in response to both IL-6 and IFN-γ (Fig. 8C), demonstrating that, in the absence of STAT3, upregulation of STAT1 signaling was not restricted to activation by IL-6R. Moreover, we found that the anti-inflammatory properties of IL-10 in suppressing LPS-mediated induction of IL-1β were conserved in STAT3-haplodeficient BMDMs, whereas these properties were abrogated in BMDMs with complete STAT3 deficiency (Fig. 8D). These results indicated that STAT3 plays a critical role in the fibroblast-activated macrophage and that incomplete inhibition attenuates macrophage activation by IL-6 and PH-Fib CM and conserves responsiveness to anti-inflammatory IL-10; however, complete deletion of STAT3 promotes macrophage activation in response to IL-6 through increased STAT1 signaling and abrogates responsiveness to anti-inflammatory IL-10.

Based on the attenuated *Arg1* expression found in PH-Fib CM–activated *C/ebpb*-deficient macrophages (Fig. 3F), we next examined the role of C/EBPβ in this STAT3-activated macrophage phenotype. *C/ebpb* mRNA was robustly expressed in mouse, rat, and bovine macrophages after exposure to bovine and human PH-Fib CM (Supplemental Fig. 4B). Importantly, PH-Fib–mediated expression of STAT3-regulated genes was significantly attenuated in macrophages with genetic deletion of *C/ebpb* (Fig. 8E).

Finally, we determined the role of HIF1 signaling in IL-6–mediated STAT3-regulated gene expression. For this purpose, we used WT BMDMs (derived from $Hif1a^{+/+}$*; LysMcre*) and $Hif1a^{-/-}$ BMDMs (derived from $Hif1a^{fl/fl}$*; LysMcre mice*) and measured gene expression of the canonical STAT3-regulated gene *Arg1* in response to IL-6. We found that IL-6–induced expression of *Arg1* was significantly increased in the presence of HIF1α stabilization with dimethyloxaloglicine, 2 μM, demonstrating that HIF1α can directly promote STAT3-regulated gene expression. Genetic absence of HIF1α significantly reduced IL-6–induced *Arg1* expression in both the presence and absence of HIF1α stabilization (Fig. 8F), demonstrating a critical role for HIF1α in regulating IL-6–mediated *Arg1* expression.

Discussion

Our studies provide evidence that, in multiple animal models and humans with PH/iPAH, macrophages accumulate specifically within the PA adventitia (a site of active vascular remodeling) (12);

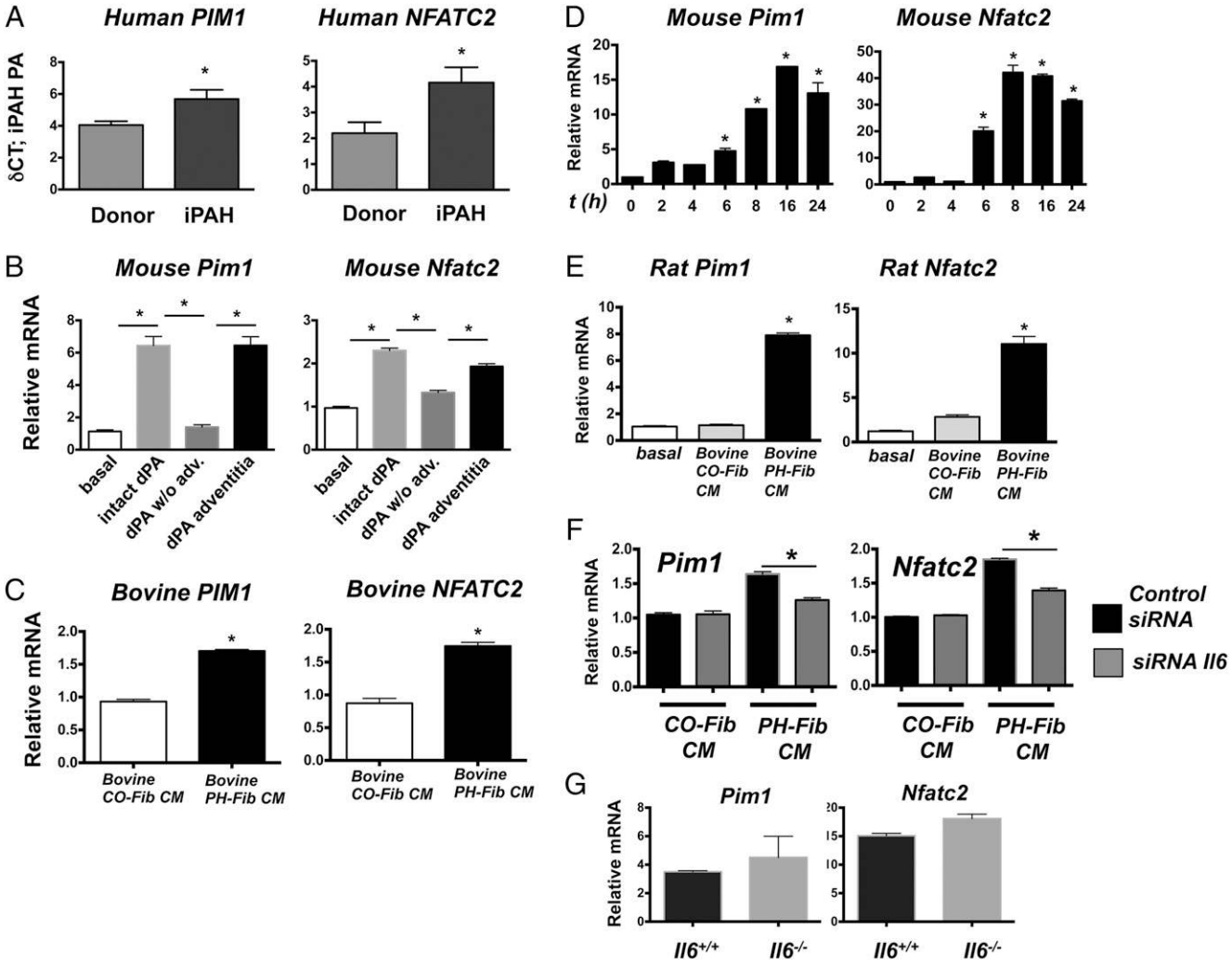

FIGURE 5. PIM1 and NFATC2 signaling is promoted in fibroblast-activated macrophages. (**A**) *PIM1* and *NFATC2* expression in laser-capture microdissected PA tissue from humans with iPAH compared with controls (iPAH $n = 8$, controls $n = 7$), expressed as δCt values normalized to expression of *PBGD*. $*p < 0.05$, unpaired two-tailed Student *t* test. (**B**) Soluble factors from the dPA adventitia (using dPA explants and 0.4-μm Transwells as in Fig. 2) induce gene expression of *Pim1* and *Nfatc2* in mouse BMDMs. Displayed is the fold induction (normalized to basal expression) of a representative PCR triplicate (average ± SEM) from one of two calves. Three dPA segments were tested from each animal; gene expression after incubation for 16 h is shown. $*p < 0.05$, one-way ANOVA. Bovine PH-Fib CM induce gene expression of *PIM1* and *NFATC2* in bovine (**C**; 16-h time point shown), mouse (**D**; time course is shown), and rat (**E**; 16-h time point is shown) BMDMs. Displayed are PCR triplicates of a representative experiment with one CO-Fib and one PH-Fib CM (mean ± SEM) normalized to *Hprt1* expression and expressed relative to basal (untreated) gene expression. These are representative of three experiments with CM from three CO-Fib and three PH-Fib cell populations on BMDMs from three animals. $*p < 0.05$, unpaired two-tailed Student *t* test. (**F**) siRNA-mediated suppression of *IL6* gene transcription in bovine PH-Fibs limits the ability of CM to induce transcription of *Pim1* and *Nfatc2* in WT mouse BMDMs. Gene expression is normalized to expression of *Hprt1* and relative to that in macrophages exposed to CM from CO-Fibs treated with control siRNA. Data are mean ± SEM from triplicate determinations and are representative of two separate experiments. $*p < 0.05$, unpaired two-tailed Student *t* test of triplicate PCR analysis. (**G**) Expression of *Pim1* and *Nfatc2* in WT and $Il6^{-/-}$ BMDMs exposed for 16 h to bovine PH-Fib CM. One representative experiment with CM from one of three PH-Fib populations was tested on BMDMs from three animals of each genotype.

these adventitial macrophages stereotypically express CD163 and CD206; the adventitial compartment is responsible for macrophage activation to this phenotype; adventitial fibroblasts are the responsible adventitial cell that mediates macrophage activation toward a previously unrecognized and distinct alternative activation phenotype; the mechanism of macrophage activation involves paracrine fibroblast–derived IL-6 and macrophage STAT3, C/EBPβ, and HIF1α signaling in the absence of IL-4/IL-13–STAT6, as well as TLR–MyD88; and targeting of C/EBPβ and HIF1α and attenuation of, but not annihilation of, STAT3, reduces macrophage activation. Based on these findings, we propose that fibroblast-mediated activation of macrophages through IL-6–STAT3 signaling towards a proremodeling phenotype (42, 43, 45, 46) is a stereotypic response pattern in vascular remodeling associated with various forms of PH. Furthermore, cooperative signaling among STAT3, HIF1α, and C/EBPβ in response to IL-6 shapes a distinct macrophage phenotype.

Considering the reported pivotal role of macrophages in PA vascular remodeling in PH (8, 24, 53), our study suggests that adventitial macrophages expressing CD163/CD206 through STAT3 signaling are critical regulators of the vascular remodeling process in PH. To our knowledge, our study is the first to show that, in vascular remodeling associated with PH, adventitial macrophages express CD163 and CD206 and that this phenotype can be induced by soluble factors generated by adventitial fibroblasts. Being that, to our knowledge, our study is the first to associate this macrophage phenotype with vascular remodeling and considering that studies examining the role of this macrophage

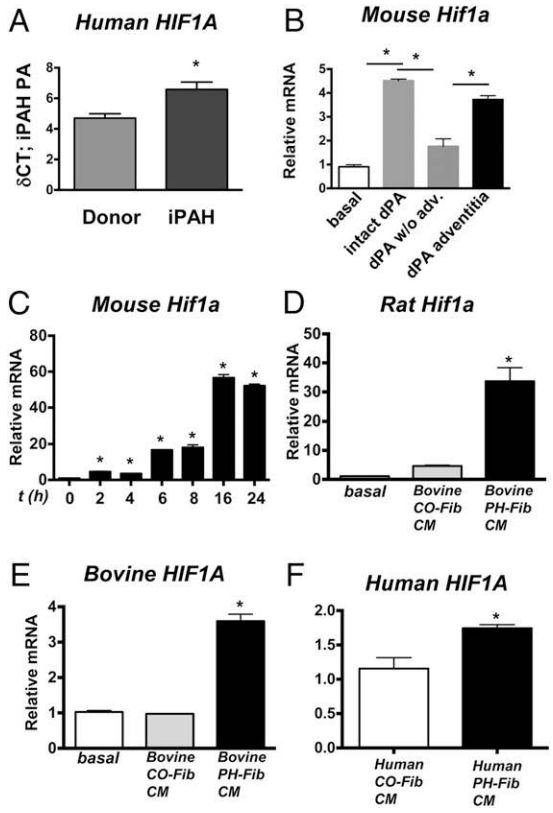

FIGURE 6. *Hif1a* is expressed in fibroblast-activated macrophages. (**A**) *HIF1a* gene expression in laser-capture microdissected PA tissue from humans with iPAH ($n = 8$) compared with controls ($n = 7$), expressed as δCt values normalized to expression of *PBGD*. (**B**) Soluble factors from the dPA adventitia (using dPA explants from PH calves and 0.4-μm Transwells, as in Fig 2) induce gene expression of *Hif1a* in mouse BMDMs. Displayed is the fold induction (normalized to basal expression) of a representative PCR triplicate (average ± SEM) from one of two calves. Three dPA segments were tested from each animal; 16-h time point is shown. Bovine PH-Fib CM induce gene expression of *Hif1a* in mouse (**C**; time course is shown), rat (**D**; 16-h time point), and bovine (**E**; 16-h time point) BMDMs. Displayed are PCR triplicates of a representative experiment with one CO-Fib and one PH-Fib CM (mean ± SEM) normalized to *Hprt1* expression and expressed relative to basal (untreated) gene expression. These are representative of three experiments with CM from three CO-Fib and three PH-Fib cell populations on BMDMs from three animals. (**F**) *HIF1A* gene expression in human THP-1 monocytes exposed to human PH-Fib CM compared with those exposed to human CO-Fib CM. Data are shown as mean ± SEM of PCR triplicates after normalization to expression of *Hprt1* and expressed relative to CO-Fib CM–induced gene expression (16-h exposure). $*p < 0.05$, unpaired two-tailed Student's *t*-test (A and F), $*p < 0.05$, one-way ANOVA (B–E).

phenotype functionally in fibrosing diseases are rare, we can only speculate with regard to its specific role in vascular remodeling. Christmann et al. (23) showed that PBMCs from patients with scleroderma-PH express higher levels of CD206 than do those from patients with scleroderma without PH and healthy controls; they correlated CD206 expression with mean PA pressures and mortality. Nakayama et al. (54) found that, of patients with scleroderma and elevated serum soluble CD163 levels, 70% had an elevated right ventricular systolic pressure on echocardiography compared with 28% of patients with normal levels. In patients with sickle cell disease and PH, soluble CD163 levels were more than twice that of sickle cell patients without PH (55).

Consistent with the restricted localization of macrophages with this phenotype to the adventitia, we found that the adventitia of the PA is the principal vascular compartment in which macrophages are activated toward this phenotype. Further, our findings demonstrate that CM from PH-Fibs fully replicates the ability of the PA adventitia to activate macrophages; thus, our study demonstrates that adventitial fibroblasts are likely the principal mediators of adventitial macrophage activation and phenotypic polarization. This finding also excludes the possibility that the activating ability of the adventitial fibroblast was an in vitro–acquired artifact; furthermore, it argues against a role for direct cell–cell contacts, including costimulatory molecules and Ag presentation. Finally, these observations justified using PH-Fib CM and naive BMDMs for further in vitro analysis of the signaling pathways that were involved in activating macrophages.

Our study unexpectedly revealed no detectable *IL4* and *IL13* mRNA or IL-4/IL-13 protein in PA tissue from iPAH patients, calves or rats with PH, or in human and bovine PH-Fibs and PH-Fib CM. Consistent with the absence of IL-4/IL-13, no STAT6 signaling was detected in macrophages in response to PA adventitia or PH-Fib CM, and the canonical STAT6-regulated genes *Chi3l3*, *Retnla*, and *Tgm2* were not expressed. The independence of this macrophage phenotype from STAT6 signaling demonstrates that these fibroblast-activated macrophages are not alternatively activated in the classical sense (19, 47). However, we found that intact PAs, PA adventitia, and PH-Fib CM induced expression of *Arg1* (which is a canonical STAT6-regulated gene) in the absence of STAT6 phosphorylation in mouse, rat, and bovine macrophages. Because Arginase1 (encoded by *Arg1*) is a macrophage product with important roles in tissue remodeling, including PH, and is thought to be a functional hallmark of AAM (48, 56), we examined the mechanism of its expression in fibroblast-activated macrophages in greater detail. *Arg1* can be induced in macrophages through multiple pathways: IL-4/IL-13–STAT6 signaling, in which C/EBPβ plays a critical role (49), as well as STAT6-independent signaling, in which intracellular microbes engage the TLR–MyD88–C/EBPβ pathway (48). This latter pathway involves generation of IL-6 in infected macrophages, which, in a paracrine fashion, induces *Arg1* through STAT3 signaling in uninfected bystander macrophages (36). Our data identify an additional pathway of *Arg1* expression in macrophages that occurs in the absence of microbial infection or TLR–MyD88 signaling and is completely independent of IL-4/IL-13–STAT6 signaling; instead, it is controlled by fibroblast-derived paracrine IL-6 and macrophage STAT3, HIF1α, and C/EBPβ. Arginase1 was shown to promote fibrosis, including that in PH-associated vascular remodeling, by providing downstream metabolites that promote cell division, collagen synthesis, and wound healing (25, 56). Higher Arginase1 levels are found in lungs of hypoxic mice (57), and Arginase1-expressing alveolar macrophages have been implicated in the pathogenesis of hypoxia-induced PH in mice (24). In contrast, macrophage Arginase1 plays neither a protective nor pathogenic role in Th2-mediated lung pathologies (58) but is important in suppression of fibrosis in Th2-mediated hepatic and intestinal pathologies (56, 59, 60). Our study proves that Arginase1 in macrophages can be expressed in the absence of microbes and Th2 responses. Thus, macrophage Arginase1 may promote or inhibit fibrosis in a disease/trigger context and organ/compartment-specific manner. Consequently, fibroblast-mediated persistent expression of Arginase1 in vascular macrophages may promote vascular remodeling in PH and possibly tissue remodeling in various pathologies in the absence of microbial triggers and Th2-mediated inflammation.

In addition to IL-4/IL-13, which can be involved in the classic Th2-mediated pulmonary vascular remodeling seen in asthma or schistosomiasis (18, 26), IL-6 plays a major role in vascular remodeling associated with certain forms of PH, as indicated by our detection of high IL-6 levels in PAs from patients with PH,

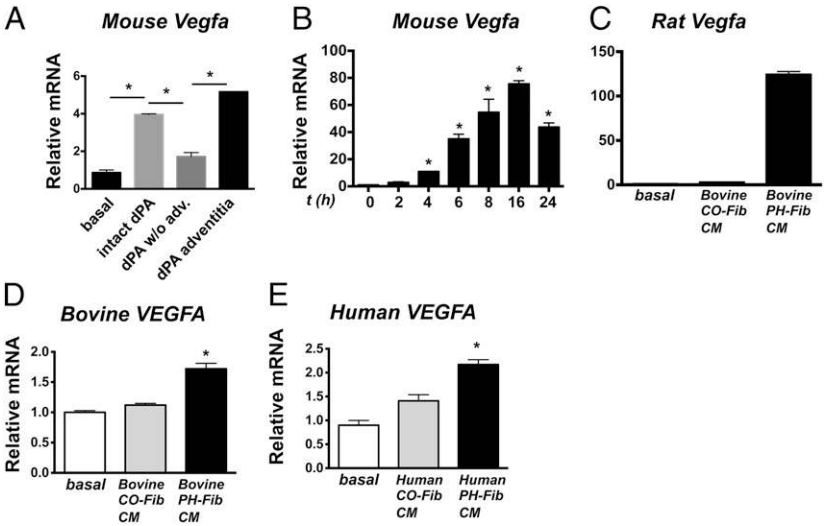

FIGURE 7. *Vegfa* is expressed in fibroblast-activated macrophages. (**A**) Soluble factors from the dPA adventitia (using dPA explants and 0.4-μm Transwells as in Fig. 2) induce gene expression of *Vegfa* in mouse BMDMs. Displayed is the fold induction (normalized to basal expression) of a representative PCR triplicate (average ± SEM) from one of two calves. Three dPA segments were tested from each animal (16-h time point). Bovine PH-Fib CM induce gene expression of *Vegfa* in mouse (**B**; time course is shown), rat (**C**; 16-h time point), and bovine (**D**; 16-h time point) BMDMs. Displayed are PCR triplicates of a representative experiment with one CO-Fib and one PH-Fib CM (mean ± SEM) normalized to *Hprt1* expression and expressed relative to basal (untreated) gene expression. These are representative of three experiments with CM from three CO-Fib and three PH-Fib cell populations on BMDMs from three animals. (**E**) *VEGFA* gene expression in human THP-1 monocytes exposed to human PH-Fib CM compared with those exposed to human CO-Fib CM. One representative experiment with CM from CO-Fibs and PH-Fibs isolated from at least three patients/controls is shown. Data were obtained 16 h after stimulation. $*p < 0.05$, ANOVA.

together with p-STAT3 and expression of canonical STAT3-regulated genes. Note that adventitial macrophages in the PA of hypoxic calves coexpressed SOCS3 and the STAT3-regulated protein CD163 and that PH-Fibs expressed high levels of IL-6. Moreover, explanted PA adventitial tissue, as well as bovine and human PH-Fib CM, induced an identical STAT3-regulated gene expression pattern in naive human, bovine, mouse, and rat macrophages. Importantly, the STAT3-regulated gene expression pattern was attenuated in macrophages in response to CM from siRNA–IL-6–treated PH-Fibs. These findings are consistent with the pivotal role of IL-6 in various mouse models of pulmonary remodeling/fibrosis, including models in which mice overexpressing IL-6 display severe hypoxia-induced PH accompanied by inflammatory vascular remodeling, whereas mice genetically deficient in IL-6 are protected from PH (30, 32).

Recent studies reported that *src*-induced STAT3–PIM1–NFACTc2 signaling enhances proliferation and resistance to apoptosis in smooth muscle cells during PH-associated vascular remodeling, although the role of IL-6 was not addressed (33, 34). In this study, we found that, consistent with the known role of IL-6 in activating STAT3 in macrophages (37), STAT3 signals in PH can be regulated through IL-6 and that PIM1 and NFACTc2 expression in macrophages can be mediated by fibroblast-derived IL-6. The incomplete attenuation of *Pim1* and *Nfatc2* expression in macrophages in response to CM from siRNA–IL-6–treated PH-Fibs raises the possibility that intracellular signaling pathways through *src* contribute to IL-6–induced STAT3 signaling in macrophages and that enhanced proliferation and apoptosis resistance in the vessel wall also are controlled by fibroblast-derived IL-6 in any IL-6–responsive cell, including fibroblasts, macrophages, endothelial cells, and smooth muscle cells. We (12) and other investigators (9) proposed that intercellular signaling pathways originating in the PA adventitia may be essential in promoting medial and intimal changes in the vascular remodeling process. The observation that expression of IL-6, STAT3, and IL-4Rα was not limited to the PA adventitia supports IL-6–STAT3 signaling as a mechanism of cross-talk between the different compartments of the vascular wall.

PH-Fib CM–activated macrophages also expressed *Hif1a* and *Vegfa*, factors critically involved in PH tissue remodeling and vascularization (61, 62). This finding led us to hypothesize that HIF1α plays a critical role in IL-6–STAT3–mediated gene expression. Thus, we tested the isolated effect of IL-6 on expression of Arginase1 in the presence or absence of HIF1α. We made the novel observation that HIF1α plays a critical role in regulating expression of Arginase1 in response to IL-6. Thus, HIF1α may fine-tune IL-6–STAT3 signaling–regulated gene expression in macrophages, as well as other cells within the vessel wall that are responsive to IL-6. Thus, because HIFα is downstream of STAT3, IL-6–induced STAT3 might serve as a central hub for the coordination of gene expression patterns that are involved in inflammation (*Hif1a, Arg1, Socs3*), remodeling (*Arg1*), metabolism (*Hif1a*), proliferation and apoptosis (*Pim1, Nfatc2*), and vascularization (*Vegfa*). Furthermore, this hypothesis is supported by the recent observation that transcription of *Vegf* can be cooperatively regulated by STAT3 and HIF1α (63, 64). Moreover, analysis of the STAT3 promoter revealed HIF1α binding sites (J.M. Poth, unpublished observations); thus, a feed-forward signaling loop between HIF1α and STAT3 might drive persistent activation of STAT3-regulated genes in response to IL-6.

Therefore, we hypothesized that genetic deficiency of STAT3 would attenuate the IL-6– and PH-Fib–activated macrophage phenotype, which would be consistent with the proposed role of STAT3 inhibition as a therapeutic approach in treating PH (33, 34, 65). We observed that activation of BMDMs with genetic haplodeficiency in *Stat3* in response to PH-Fib CM and rIL-6 was attenuated, consistent with a critical role for STAT3 in promoting this macrophage phenotype. However, we also made the important observation that complete genetic blockade of STAT3 signaling in IL-6– and PH-Fib–stimulated macrophages resulted in increased activation (increase in expression of STAT3-regulated genes), which was associated with increased and prolonged STAT1

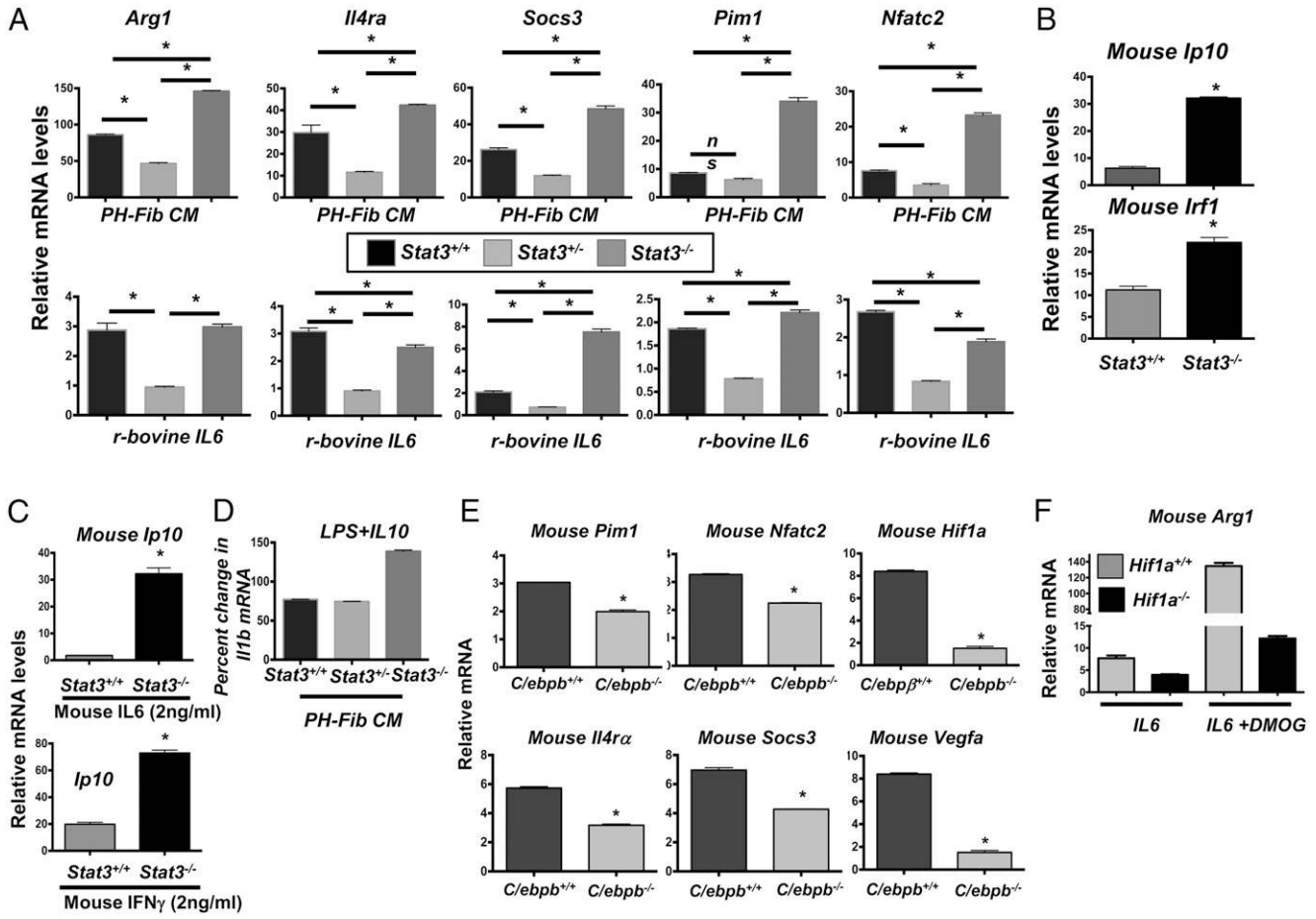

FIGURE 8. STAT3, C/EBPb, and HIF1α are critical regulators of fibroblast-mediated macrophage activation. (**A**) Transcription of *Arg1*, *Il4ra*, *Socs3*, *Pim1*, and *Nfatc2* in BMDMs from *Stat3*$^{fl/fl}$*;Tie2cre* (designated *Stat3*$^{-/-}$) mice compared with BMDMs from WT mice (*Stat3*$^{+/+}$) and from *Stat3*$^{fl/+}$*; Tie2cre* (designated *Stat3*$^{+/-}$) mice in response to bovine PH-Fib CM (*upper panel*) and bovine rIL-6 (2 ng/ml, *lower panel*) after stimulation for 16 h. (**B**) STAT1 target gene expression (*Ip10* and *Irf1*) in *Stat3*$^{-/-}$ BMDMs compared with WT (*Stat3*$^{+/+}$) BMDMs in response to bovine PH-Fib CM after stimulation for 16 h. (**C**) STAT1 target gene expression (*Ip10*) in response to stimulation with mouse rIL-6 (*upper panel*) or mouse rIFN-γ (*lower panel*) in *Stat3*$^{-/-}$ BMDMs compared with WT BMDMs. (**D**) Percentage gene expression of *Il1b* in WT, Stat3$^{+/-}$, and Stat3$^{-/-}$ BMDMs in response to LPS (100 ng/ml)+IL-10 (10 ng/ml) compared with LPS (100 ng/ml) alone (set as 100%) after 16 h of incubation. (**E**) Gene expression of *Pim1*, *Nfatc2*, *Hif1a*, *Il4ra*, *Socs3*, and *Vegfa* in *C/ebpb*$^{-/-}$ mouse BMDMs compared with WT BMDMs in response to bovine PH-Fib CM after 16 h of stimulation. (**F**) Expression of *Arg1* in *LysMcre* (designated *Hif1a*$^{+/+}$) mice and *Hif1a*$^{fl/fl}$*;LysMcre* (designated *Hif1a*$^{-/-}$) mice BMDMs in response to mouse rIL-6 (after stimulation for 16 h) in the presence or absence of HIF1α stabilization with DMOG. Data are from PCR triplicates and are representative of results obtained from at least two PH-Fib isolates and BMDMs from two animals. *$p < 0.05$, unpaired two-tailed Student *t* test.

phosphorylation and increased expression of canonical STAT1-regulated proinflammatory genes. These findings prompted the question of how STAT3-regulated genes can be upregulated in the absence of STAT3 protein. A previous study demonstrated that genetic deletion of STAT3 in IL-6–stimulated mouse fibroblasts also resulted in increased and prolonged p-STAT1 signaling and upregulation of STAT1 and STAT3 target genes (i.e., Arginase1) (52). These findings, together with our results, demonstrate that, in the complete absence of STAT3, IL-6 signaling enhances expression of both STAT1- and STAT3-regulated genes in fibroblasts and macrophages through increased and prolonged STAT1 signaling. Similarly, a previous study demonstrated that, in the genetic absence of STAT1, macrophages express increased amounts of STAT3-regulated genes (66). These studies, together with our findings, highlight that STAT1 and STAT3 can cross-regulate gene expression. In addition, our data also demonstrate that anti-inflammatory IL-10 signaling is abrogated in the complete absence of STAT3 but is fully preserved in the incomplete inhibition of STAT3, findings that are consistent with the reported nonredundant role of STAT3 in mediating the IL-10–regulated anti-inflammatory response in macrophages and the principal role for macrophages in mediating IL-10–STAT3 anti-inflammatory signaling (67). Thus, our data are consistent with reported STAT3-inhibition studies that show attenuation of PH in animal models, but they also suggest that complete STAT3 blockade may render any IL-6-responsive cell within the vessel wall, including fibroblasts, refractory to anti-inflammatory IL-10 and promote persistent proinflammatory STAT1-mediated activation in response to paracrine IL-6 (33, 34). Thus, it remains to be determined whether STAT3 blockade is a safe approach for treatment of PH.

We next focused on signaling pathways downstream of STAT3 that were involved in promoting this macrophage phenotype and, thus, could be additional candidate therapeutic targets. We found that genetic absence of C/EBPβ or HIF1α (both transcription factors associated with proinflammatory activation of macrophages and both STAT3 target genes) attenuated macrophage activation in response to IL-6 and PH-Fib CM, which was paralleled by attenuated transcription of STAT3 target genes. This finding is consistent with the reported synergistic function of C/EBPβ and HIF1α with STATs (49, 63, 64, 68), as well as with studies in-

dicating a role for C/EBPβ in regulating macrophage activation in obesity, wound healing, and ischemic heart injury (36, 48, 49, 69–71). Importantly, unlike the consequences of completely blocking STAT3, the IL-10–mediated anti-inflammatory response is fully functional in the absence of C/EBPβ and HIF1α (K.C. El Kasmi and P.J. Murray, unpublished observations; P.J. Murray, personal communication). Thus, targeting C/EBPβ and/or HIF1α may effectively mitigate IL-6–mediated remodeling in various pathologies, such as PH and rheumatoid arthritis. Analysis of the therapeutic potential of STAT3 versus C/EBPβ or HIF1α inhibition on vascular remodeling awaits the examination of animal models with cell type–specific ablation of STAT3, HIF1α, and C/EBPβ.

Collectively, our data identify an intercellular signaling mechanism in the PA adventitia that is controlled by fibroblast-mediated signaling in various species and forms of PH and that shapes macrophage differentiation toward a distinct phenotype critically regulated through IL-6, STAT3, HIF1α, and C/EBPβ in the absence of pathogens, danger signals, and Th2 cytokines. Based on the independence of this macrophage phenotype from TLR–MyD88 and STAT6 signaling and considering the critical role of STAT3 signaling, together with the role of fibroblast-generated paracrine signals, chiefly IL-6, in controlling this phenotype, we conclude that these STAT3-activated macrophages portray a distinct functional phenotype representing its own category of macrophage activation that is crucial in pathological tissue remodeling. This intercellular signaling axis in IL-6–, fibroblast-, and STAT3-activated macrophages might be important in other chronic fibrotic inflammatory conditions that occur in the absence of Th2-derived cytokines and pathogens, such as scleroderma, rheumatoid arthritis, acute respiratory distress syndrome, and fibrotic lung disease.

Acknowledgments

We thank Dr. Peter Murray for providing the STAT3-deficient bone marrow and for critically reviewing the manuscript. We acknowledge the technical assistance of Amanda L. Flockton and B. Alexandre McKeon. We thank Dr. Michael Yeager and Kelly Colvin for help with immunostaining PAs from hypoxic and MCT-treated rats. Confocal imaging was performed at Advance Light Microscopy Core, University of Colorado Denver.

Disclosures

The authors have no financial conflicts of interest.

References

1. Morrell, N. W., S. L. Archer, A. Defelice, S. Evans, M. Fiszman, T. Martin, M. Saulnier, M. Rabinovitch, R. Schermuly, D. Stewart, et al. 2013. Anticipated classes of new medications and molecular targets for pulmonary arterial hypertension. Pulm. Circ. 3: 226–244.
2. Price, L. C., S. J. Wort, F. Perros, P. Dorfmüller, A. Huertas, D. Montani, S. Cohen-Kaminsky, and M. Humbert. 2012. Inflammation in pulmonary arterial hypertension. *Chest* 141: 210–221.
3. Savai, R., S. S. Pullamsetti, J. Kolbe, E. Bieniek, R. Voswinckel, L. Fink, A. Scheed, C. Ritter, B. K. Dahal, A. Vater, et al. 2012. Immune and inflammatory cell involvement in the pathology of idiopathic pulmonary arterial hypertension. *Am. J. Respir. Crit. Care Med.* 186: 897–908.
4. Stacher, E., B. B. Graham, J. M. Hunt, A. Gandjeva, S. D. Groshong, V. V. McLaughlin, M. Jessup, W. E. Grizzle, M. A. Aldred, C. D. Cool, and R. M. Tuder. 2012. Modern age pathology of pulmonary arterial hypertension. *Am. J. Respir. Crit. Care Med.* 186: 261–272.
5. Stenmark, K. R., B. Meyrick, N. Galie, W. J. Mooi, and I. F. McMurtry. 2009. Animal models of pulmonary arterial hypertension: the hope for etiological discovery and pharmacological cure. *Am. J. Physiol. Lung Cell. Mol. Physiol.* 297: L1013–L1032.
6. Tuder, R. M., and N. F. Voelkel. 1998. Pulmonary hypertension and inflammation. *J. Lab. Clin. Med.* 132: 16–24.
7. Tuder, R. M., S. L. Archer, P. Dorfmüller, S. C. Erzurum, C. Guignabert, E. Michelakis, M. Rabinovitch, R. Schermuly, K. R. Stenmark, and N. W. Morrell. 2013. Relevant issues in the pathology and pathobiology of pulmonary hypertension. *J. Am. Coll. Cardiol.* 62(25, Suppl): D4–D12.
8. Frid, M. G., J. A. Brunetti, D. L. Burke, T. C. Carpenter, N. J. Davie, J. T. Reeves, M. T. Roedersheimer, N. van Rooijen, and K. R. Stenmark. 2006. Hypoxia-induced pulmonary vascular remodeling requires recruitment of circulating mesenchymal precursors of a monocyte/macrophage lineage. *Am. J. Pathol.* 168: 659–669.
9. Hassoun, P. M., L. Mouthon, J. A. Barberà, S. Eddahibi, S. C. Flores, F. Grimminger, P. L. Jones, M. L. Maitland, E. D. Michelakis, N. W. Morrell, et al. 2009. Inflammation, growth factors, and pulmonary vascular remodeling. *J. Am. Coll. Cardiol.* 54(1, Suppl.): S10–S19.
10. Stenmark, K. R., M. G. Frid, M. Yeager, M. Li, S. Riddle, T. McKinsey, and K. C. El Kasmi. 2012. Targeting the adventitial microenvironment in pulmonary hypertension: A potential approach to therapy that considers epigenetic change. Pulm. Circ. 2: 3–14.
11. Stenmark, K. R., E. Nozik-Grayck, E. Gerasimovskaya, A. Anwar, M. Li, S. Riddle, and M. Frid. 2011. The adventitia: Essential role in pulmonary vascular remodeling. *Compr. Physiol.* 1: 141–161.
12. Stenmark, K. R., M. E. Yeager, K. C. El Kasmi, E. Nozik-Grayck, E. V. Gerasimovskaya, M. Li, S. R. Riddle, and M. G. Frid. 2013. The adventitia: essential regulator of vascular wall structure and function. *Annu. Rev. Physiol.* 75: 23–47.
13. Anwar, A., M. Li, M. G. Frid, B. Kumar, E. V. Gerasimovskaya, S. R. Riddle, B. A. McKeon, R. Thukaram, B. O. Meyrick, M. A. Fini, and K. R. Stenmark. 2012. Osteopontin is an endogenous modulator of the constitutively activated phenotype of pulmonary adventitial fibroblasts in hypoxic pulmonary hypertension. *Am. J. Physiol. Lung Cell. Mol. Physiol.* 303: L1–L11.
14. Das, M., N. Burns, S. J. Wilson, W. M. Zawada, and K. R. Stenmark. 2008. Hypoxia exposure induces the emergence of fibroblasts lacking replication repressor signals of PKCzeta in the pulmonary artery adventitia. *Cardiovasc. Res.* 78: 440–448.
15. Panzhinskiy, E., W. M. Zawada, K. R. Stenmark, and M. Das. 2012. Hypoxia induces unique proliferative response in adventitial fibroblasts by activating PDGFβ receptor-JNK1 signalling. *Cardiovasc. Res.* 95: 356–365.
16. Wang, D., H. Zhang, M. Li, M. G. Frid, A. R. Flockton, B. A. McKeon, M. E. Yeager, M. A. Fini, N. W. Morrell, S. S. Pullamsetti, et al. 2014. MicroRNA-124 controls the proliferative, migratory, and inflammatory phenotype of pulmonary vascular fibroblasts. *Circ. Res.* 114: 67–78.
17. Li, M., S. R. Riddle, M. G. Frid, K. C. El Kasmi, T. A. McKinsey, R. J. Sokol, D. Strassheim, B. Meyrick, M. E. Yeager, A. R. Flockton, et al. 2011. Emergence of fibroblasts with a proinflammatory epigenetically altered phenotype in severe hypoxic pulmonary hypertension. *J. Immunol.* 187: 2711–2722.
18. Duffield, J. S., M. Lupher, V. J. Thannickal, and T. A. Wynn. 2013. Host responses in tissue repair and fibrosis. *Annu. Rev. Pathol.* 8: 241–276.
19. Murray, P. J., and T. A. Wynn. 2011. Protective and pathogenic functions of macrophage subsets. *Nat. Rev. Immunol.* 11: 723–737.
20. Wynn, T. A., and L. Barron. 2010. Macrophages: master regulators of inflammation and fibrosis. *Semin. Liver Dis.* 30: 245–257.
21. Angelini, D. J., Q. Su, K. Yamaji-Kegan, C. Fan, X. Teng, P. M. Hassoun, S. C. Yang, H. C. Champion, R. M. Tuder, and R. A. Johns. 2009. Resistin-like molecule-beta in scleroderma-associated pulmonary hypertension. *Am. J. Respir. Cell Mol. Biol.* 41: 553–561.
22. Yamaji-Kegan, K., Q. Su, D. J. Angelini, A. C. Myers, C. Cheadle, and R. A. Johns. 2010. Hypoxia-induced mitogenic factor (HIMF/FIZZ1/RELMalpha) increases lung inflammation and activates pulmonary microvascular endothelial cells via an IL-4-dependent mechanism. *J. Immunol.* 185: 5539–5548.
23. Christmann, R. B., E. Hayes, S. Pendergrass, C. Padilla, G. Farina, A. J. Affandi, M. L. Whitfield, H. W. Farber, and R. Lafyatis. 2011. Interferon and alternative activation of monocyte/macrophages in systemic sclerosis-associated pulmonary arterial hypertension. *Arthritis Rheum.* 63: 1718–1728.
24. Vergadi, E., M. S. Chang, C. Lee, O. D. Liang, X. Liu, A. Fernandez-Gonzalez, S. A. Mitsialis, and S. Kourembanas. 2011. Early macrophage recruitment and alternative activation are critical for the later development of hypoxia-induced pulmonary hypertension. *Circulation* 123: 1986–1995.
25. Wynn, T. A. 2004. Fibrotic disease and the T(H)1/T(H)2 paradigm. *Nat. Rev. Immunol.* 4: 583–594.
26. Graham, B. B., J. Chabon, R. Kumar, E. Kolosionek, L. Gebreab, E. Debella, M. Edwards, K. Diener, T. Shade, G. Bifeng, et al. 2013. Protective role of IL-6 in vascular remodeling in Schistosoma pulmonary hypertension. *Am. J. Respir. Cell Mol. Biol.* 49: 951–959.
27. Knight, D. A., M. Ernst, G. P. Anderson, Y. P. Moodley, and S. E. Mutsaers. 2003. The role of gp130/IL-6 cytokines in the development of pulmonary fibrosis: critical determinants of disease susceptibility and progression? *Pharmacol. Ther.* 99: 327–338.
28. Natsume, M., H. Tsuji, A. Harada, M. Akiyama, T. Yano, H. Ishikura, I. Nakanishi, K. Matsushima, S. Kaneko, and N. Mukaida. 1999. Attenuated liver fibrosis and depressed serum albumin levels in carbon tetrachloride-treated IL-6-deficient mice. *J. Leukoc. Biol.* 66: 601–608.
29. Ash, Z., and P. Emery. 2012. The role of tocilizumab in the management of rheumatoid arthritis. *Expert Opin. Biol. Ther.* 12: 1277–1289.
30. Steiner, M. K., O. L. Syrkina, N. Kolliputi, E. J. Mark, C. A. Hales, and A. B. Waxman. 2009. Interleukin-6 overexpression induces pulmonary hypertension. Circ. Res. 104: 236–244, 28p following 244.
31. Soon, E., A. M. Holmes, C. M. Treacy, N. J. Doughty, L. Southgate, R. D. Machado, R. C. Trembath, S. Jennings, L. Barker, P. Nicklin, et al. 2010. Elevated levels of inflammatory cytokines predict survival in idiopathic and familial pulmonary arterial hypertension. *Circulation* 122: 920–927.
32. Savale, L., L. Tu, D. Rideau, M. Izziki, B. Maitre, S. Adnot, and S. Eddahibi. 2009. Impact of interleukin-6 on hypoxia-induced pulmonary hypertension and lung inflammation in mice. *Respir. Res.* 10: 6.
33. Paulin, R., A. Courboulin, J. Meloche, V. Mainguy, E. Dumas de la Roque, N. Saksouk, J. Côté, S. Provencher, M. A. Sussman, and S. Bonnet. 2011. Signal

transducers and activators of transcription-3/pim1 axis plays a critical role in the pathogenesis of human pulmonary arterial hypertension. *Circulation* 123: 1205–1215.
34. Paulin, R., J. Meloche, M. H. Jacob, M. Bisserier, A. Courboulin, and S. Bonnet. 2011. Dehydroepiandrosterone inhibits the Src/STAT3 constitutive activation in pulmonary arterial hypertension. *Am. J. Physiol. Heart Circ. Physiol.* 301: H1798–H1809.
35. Xue, J., S. V. Schmidt, J. Sander, A. Draffehn, W. Krebs, I. Quester, D. De Nardo, T. D. Gohel, M. Emde, L. Schmidleithner, et al. 2014. Transcriptome-based network analysis reveals a spectrum model of human macrophage activation. *Immunity* 40: 274–288.
36. Qualls, J. E., G. Neale, A. M. Smith, M. S. Koo, A. A. DeFreitas, H. Zhang, G. Kaplan, S. S. Watowich, and P. J. Murray. 2010. Arginine usage in mycobacteria-infected macrophages depends on autocrine-paracrine cytokine signaling. *Sci. Signal.* 3: ra62.
37. El Kasmi, K. C., J. Holst, M. Coffre, L. Mielke, A. de Pauw, N. Lhocine, A. M. Smith, R. Rutschman, D. Kaushal, Y. Shen, et al. 2006. General nature of the STAT3-activated anti-inflammatory response. *J. Immunol.* 177: 7880–7888.
38. Lang, R., A. L. Pauleau, E. Parganas, Y. Takahashi, J. Mages, J. N. Ihle, R. Rutschman, and P. J. Murray. 2003. SOCS3 regulates the plasticity of gp130 signaling. *Nat. Immunol.* 4: 546–550.
39. Fielding, C. A., G. W. Jones, R. M. McLoughlin, L. McLeod, V. J. Hammond, J. Uceda, A. S. Williams, M. Lambie, T. L. Foster, C. T. Liao, et al. 2014. Interleukin-6 signaling drives fibrosis in unresolved inflammation. *Immunity* 40: 40–50.
40. Humbert, M., G. Monti, F. Brenot, O. Sitbon, A. Portier, L. Grangeot-Keros, P. Duroux, P. Galanaud, G. Simonneau, and D. Emilie. 1995. Increased interleukin-1 and interleukin-6 serum concentrations in severe primary pulmonary hypertension. *Am. J. Respir. Crit. Care Med.* 151: 1628–1631.
41. Yoshio, T., J. I. Masuyama, N. Kohda, D. Hirata, H. Sato, M. Iwamoto, A. Mimori, A. Takeda, S. Minota, and S. Kano. 1997. Association of interleukin 6 release from endothelial cells and pulmonary hypertension in SLE. *J. Rheumatol.* 24: 489–495.
42. Ikezumi, Y., T. Suzuki, T. Karasawa, H. Hasegawa, T. Yamada, N. Imai, I. Narita, H. Kawachi, K. R. Polkinghorne, D. J. Nikolic-Paterson, and M. Uchiyama. 2011. Identification of alternatively activated macrophages in new-onset paediatric and adult immunoglobulin A nephropathy: potential role in mesangial matrix expansion. *Histopathology* 58: 198–210.
43. Mathai, S. K., M. Gulati, X. Peng, T. R. Russell, A. C. Shaw, A. N. Rubinowitz, L. A. Murray, J. M. Siner, D. E. Antin-Ozerkis, R. R. Montgomery, et al. 2010. Circulating monocytes from systemic sclerosis patients with interstitial lung disease show an enhanced profibrotic phenotype. *Lab. Invest.* 90: 812–823.
44. Weaver, L. K., P. A. Pioli, K. Wardwell, S. N. Vogel, and P. M. Guyre. 2007. Up-regulation of human monocyte CD163 upon activation of cell-surface Toll-like receptors. *J. Leukoc. Biol.* 81: 663–671.
45. Higashi-Kuwata, N., T. Makino, Y. Inoue, M. Takeya, and H. Ihn. 2009. Alternatively activated macrophages (M2 macrophages) in the skin of patient with localized scleroderma. *Exp. Dermatol.* 18: 727–729.
46. Bacci, M., A. Capobianco, A. Monno, L. Cottone, F. Di Puppo, B. Camisa, M. Mariani, C. Brignole, M. Ponzoni, S. Ferrari, et al. 2009. Macrophages are alternatively activated in patients with endometriosis and required for growth and vascularization of lesions in a mouse model of disease. *Am. J. Pathol.* 175: 547–556.
47. Gordon, S. 2003. Alternative activation of macrophages. *Nat. Rev. Immunol.* 3: 23–35.
48. El Kasmi, K. C., J. E. Qualls, J. T. Pesce, A. M. Smith, R. W. Thompson, M. Henao-Tamayo, R. J. Basaraba, T. König, U. Schleicher, M. S. Koo, et al. 2008. Toll-like receptor-induced arginase 1 in macrophages thwarts effective immunity against intracellular pathogens. *Nat. Immunol.* 9: 1399–1406.
49. Gray, M. J., M. Poljakovic, D. Kepka-Lenhart, and S. M. Morris, Jr. 2005. Induction of arginase I transcription by IL-4 requires a composite DNA response element for STAT6 and C/EBPbeta. *Gene* 353: 98–106.
50. Dang, E. V., J. Barbi, H. Y. Yang, D. Jinasena, H. Yu, Y. Zheng, Z. Bordman, J. Fu, Y. Kim, H. R. Yen, et al. 2011. Control of T(H)17/T(reg) balance by hypoxia-inducible factor 1. *Cell* 146: 772–784.
51. Takeda, K., K. Noguchi, W. Shi, T. Tanaka, M. Matsumoto, N. Yoshida, T. Kishimoto, and S. Akira. 1997. Targeted disruption of the mouse Stat3 gene leads to early embryonic lethality. *Proc. Natl. Acad. Sci. USA* 94: 3801–3804.
52. Costa-Pereira, A. P., S. Tininini, B. Strobl, T. Alonzi, J. F. Schlaak, H. Is'harc, I. Gesualdo, S. J. Newman, I. M. Kerr, and V. Poli. 2002. Mutational switch of an IL-6 response to an interferon-gamma-like response. *Proc. Natl. Acad. Sci. USA* 99: 8043–8047.
53. Tuder, R. M., E. Stacher, J. Robinson, R. Kumar, and B. B. Graham. 2013. Pathology of pulmonary hypertension. *Clin. Chest Med.* 34: 639–650.
54. Nakayama, W., M. Jinnin, K. Makino, I. Kajihara, T. Makino, S. Fukushima, Y. Inoue, and H. Ihn. 2012. Serum levels of soluble CD163 in patients with systemic sclerosis. *Rheumatol. Int.* 32: 403–407.
55. Tantawy, A. A., A. A. Adly, and E. A. Ismail. 2012. Soluble CD163 in young sickle cell disease patients and their trait siblings: a biomarker for pulmonary hypertension and vaso-occlusive complications. *Blood Coagul. Fibrinolysis* 23: 640–648.
56. Campbell, L., C. R. Saville, P. J. Murray, S. M. Cruickshank, and M. J. Hardman. 2013. Local arginase 1 activity is required for cutaneous wound healing. *J. Invest. Dermatol.* 133: 2461–2470.
57. Jin, Y., T. J. Calvert, B. Chen, L. G. Chicoine, M. Joshi, J. A. Bauer, Y. Liu, and L. D. Nelin. 2010. Mice deficient in Mkp-1 develop more severe pulmonary hypertension and greater lung protein levels of arginase in response to chronic hypoxia. *Am. J. Physiol. Heart Circ. Physiol.* 298: H1518–H1528.
58. Barron, L., A. M. Smith, K. C. El Kasmi, J. E. Qualls, X. Huang, A. Cheever, L. A. Borthwick, M. S. Wilson, P. J. Murray, and T. A. Wynn. 2013. Role of arginase 1 from myeloid cells in th2-dominated lung inflammation. *PLoS ONE* 8: e61961.
59. Herbert, D. R., C. Hölscher, M. Mohrs, B. Arendse, A. Schwegmann, M. Radwanska, M. Leeto, R. Kirsch, P. Hall, H. Mossmann, et al. 2004. Alternative macrophage activation is essential for survival during schistosomiasis and downmodulates T helper 1 responses and immunopathology. *Immunity* 20: 623–635.
60. Herbert, D. R., T. Orekov, A. Roloson, M. Ilies, C. Perkins, W. O'Brien, S. Cederbaum, D. W. Christianson, N. Zimmermann, M. E. Rothenberg, and F. D. Finkelman. 2010. Arginase I suppresses IL-12/IL-23p40-driven intestinal inflammation during acute schistosomiasis. *J. Immunol.* 184: 6438–6446.
61. Voelkel, N. F., R. W. Vandivier, and R. M. Tuder. 2006. Vascular endothelial growth factor in the lung. *Am. J. Physiol. Lung Cell. Mol. Physiol.* 290: L209–L221.
62. Semenza, G. L. 2011. Oxygen sensing, homeostasis, and disease. *N. Engl. J. Med.* 365: 537–547.
63. Jung, J. E., H. G. Lee, I. H. Cho, D. H. Chung, S. H. Yoon, Y. M. Yang, J. W. Lee, S. Choi, J. W. Park, S. K. Ye, and M. H. Chung. 2005. STAT3 is a potential modulator of HIF-1-mediated VEGF expression in human renal carcinoma cells. FASEB J. 19: 1296–1298.
64. Xu, Q., J. Briggs, S. Park, G. Niu, M. Kortylewski, S. Zhang, T. Gritsko, J. Turkson, H. Kay, G. L. Semenza, et al. 2005. Targeting Stat3 blocks both HIF-1 and VEGF expression induced by multiple oncogenic growth signaling pathways. *Oncogene* 24: 5552–5560.
65. Paulin, R., J. Meloche, and S. Bonnet. 2012. STAT3 signaling in pulmonary arterial hypertension. *JAK-STAT* 1: 223–233.
66. Ramana, C. V., A. Kumar, and R. Enelow. 2005. Stat1-independent induction of SOCS-3 by interferon-gamma is mediated by sustained activation of Stat3 in mouse embryonic fibroblasts. *Biochem. Biophys. Res. Commun.* 327: 727–733.
67. Akira, S. 2000. Roles of STAT3 defined by tissue-specific gene targeting. *Oncogene* 19: 2607–2611.
68. Pauleau, A. L., R. Rutschman, R. Lang, A. Pernis, S. S. Watowich, and P. J. Murray. 2004. Enhancer-mediated control of macrophage-specific arginase I expression. *J. Immunol.* 172: 7565–7573.
69. Rahman, S. M., R. C. Janssen, M. Choudhury, K. C. Baquero, R. M. Aikens, B. A. de la Houssaye, and J. E. Friedman. 2012. CCAAT/enhancer-binding protein β (C/EBPβ) expression regulates dietary-induced inflammation in macrophages and adipose tissue in mice. *J. Biol. Chem.* 287: 34349–34360.
70. Ruffell, D., F. Mourkioti, A. Gambardella, P. Kirstetter, R. G. Lopez, N. Rosenthal, and C. Nerlov. 2009. A CREB-C/EBPbeta cascade induces M2 macrophage-specific gene expression and promotes muscle injury repair. *Proc. Natl. Acad. Sci. USA* 106: 17475–17480.
71. Huang, G. N., J. E. Thatcher, J. McAnally, Y. Kong, X. Qi, W. Tan, J. M. DiMaio, J. F. Amatruda, R. D. Gerard, J. A. Hill, et al. 2012. C/EBP transcription factors mediate epicardial activation during heart development and injury. *Science* 338: 1599–1603.